
Considerations for Successful Encapsulated β -Cell Therapy

2

Christopher G. Thanos, Jason L. Gaglia,
and Felicia W. Pagliuca

Introduction

Type 1 diabetes (T1D) is a disease of insulin insufficiency that can be clinically managed with delivery of various exogenous insulin formulations, typically via subcutaneous injection or infusion. Otherwise, insufficient insulin can lead to acute complications including ketoacidosis or chronic complications including nephropathy, retinopathy, macular edema, neuropathy, and macrovascular disease. With intensive insulin therapy, risks of developing these complications can be reduced [1]. However, the burden on the patient makes long-term compliance a difficult proposition, often resulting in increasingly poor control and secondary health issues [2]. One of the greatest concerns of tight glycemic control is the possibility of life-threatening iatrogenic hypoglycemia. In clinical practice, approximately 90% of all patients self-administering insulin have experienced some degree of hypoglycemia [3]. Once plasma glucose falls below about 70 mg/dL, a cascade of released hormones leads to reduced glucose uptake in peripheral tissues [4] and initiation of counter regulatory mechanisms that are observed over hours. Hypoglycemia can lead to seizures, coma, and death [5].

The pharmacological challenge of treating T1D involves utilization of insulin, a drug with a rather narrow and variable therapeutic window, to achieve

C.G. Thanos, Ph.D. (✉)

VP Delivery R&D, Semma Therapeutics, 117 Chapman St., Providence, RI 02905, USA
e-mail: c.thanos@semma-tx.com

J.L. Gaglia, M.D., M.M.Sc.

Section on Immunobiology, Joslin Diabetes Center,
One Joslin Place, Boston, MA 02215, USA
e-mail: jason.gaglia@joslin.harvard.edu

F.W. Pagliuca, Ph.D.

VP Cell Biology R&D, Semma Therapeutics, 450 Kendall St, Cambridge, MA 02142, USA
e-mail: f.pagliuca@semma-tx.com

normoglycemia, which under normal physiologic conditions involves the interplay of multiple hormone mediators, activity, and carbohydrate intake as major factors. Intravenous insulin as is delivered by the pancreas has much more rapid kinetics than insulin that is subcutaneously delivered. The variable requirements for insulin delivery in T1D may be better suited for delivery systems that can respond dynamically and that incorporate glucose sensing and control of insulin release in a way that behaves more similarly to the innate pancreas. Since the timing and magnitude of insulin dosing is dependent on plasma glucose, the system must be able to couple the two activities (sensing and delivery) without significant delays due to secretion, diffusion, uptake, or other transport-limiting phenomena. Many strategies for such systems have been evaluated, including pulsatile-release polymeric microspheres [6], multiphasic insulin conjugates [7, 8], insulin pumps [9], naked islet therapy [10], and the bioartificial pancreas [11, 12].

In September of 2016, Medtronic announced FDA approval of its automated insulin delivery device for T1D [12], the first approval of its kind. The MiniMed 670G hybrid closed-loop system measures glucose every 5 min through a body-attached sensor and delivers the appropriate amount of insulin to the subcutaneous space with an external insulin pump. This closed-loop system operates within limits defined by an algorithm with the assistance of patient inputs signaling timing of meals. The technology is particularly compelling because it can control fasting glucose with minimal patient input, protecting against unaware hypoglycemia throughout the night. The device was evaluated in clinical trials in 123 patients for 3 months, with no episodes of extreme hypoglycemia or ketoacidosis, although 24 severe hyperglycemia events were reported [13].

With this significant success using a completely artificial closed-loop system, the technology has advanced through various failure modes that have plagued its development, including blockage, sensor fouling, and insulin stability issues [14], as well as poorly predictive compensation for onboard insulin [15]. Even with pump-based insulin delivery at this advanced state, a monohormonal approach may not be sufficient to completely eradicate unaware hypoglycemia. The device's algorithm that controls insulin delivery is the only means by which glycemia is regulated, while under normal physiologic conditions during hypoglycemia [16], the alpha cells of the endocrine pancreas secrete glucagon to mobilize glycogen stored in the liver into the bloodstream as glucose. Dual hormonal therapies have been evaluated [17], and such closed-loop systems are in development [9].

The complex activities of the endocrine pancreas may be best recapitulated in a biological system wherein islet or islet-like tissue is placed within an environment in the patient that promotes viability and function through engraftment, diffusion, or integration with the host.

Primary islets from human or animal origin have been used in this role [18], but recently, islet-like tissue derived from stem cells has been developed to a level of functionality and safety that enables its use in commercial development. This chapter will detail the development of cell-based therapies for T1D, with a specific focus on the bioartificial pancreas (cells encapsulated in biomaterials) and the emerging

prospect of stem cell-derived islet-like tissue as a functional and renewable cell source.

Islet Transplantation

Clinical islet transplantation has been in practice for decades now as a therapy for T1D [18]. Originally envisioned as a panacea limited only by the availability of human cadaveric islets, a commercially viable cell therapy for T1D has remained an elusive target due in large part to the mass and metabolic demands of the β -cells required for insulin therapy. The diffusive constraints of the encapsulation systems employed to deliver islets, the variability in the quality and performance of cadaveric islets, and the host response to the encapsulation materials and secreted contents are all additional compounding factors that impact the success of the graft by activating elements of the immune system.

Portal delivery of naked islets with immunosuppression but without encapsulation, as performed in the Clinical Islet Transplantation (CIT) Consortium and the earlier Edmonton Protocol [19, 20], is perhaps the most direct way to introduce beta cells into organ parenchyma. In these studies, human cadaveric islets are infused directly into the portal vein, where they travel into the small sinusoids of the liver vasculature. This transplant site provides direct access to oxygen and nutrients in the blood while minimizing travel to distant sites through physical entrapment within the tissue. However, it is estimated that of the infused islets, only 10–20% survive the immediate posttransplant period [21]. Still, in select cases, these marginal beta cell masses have been sufficient to maintain euglycemia.

In the CIT-07 clinical trial [19], 48 subjects were implanted with an average of about 800,000 IEQ with about half of the group receiving a second transplant. Patients were immunosuppressed acutely with sirolimus (rapamycin), tacrolimus, etanercept (a TNF inhibitor), and rabbit antithymocyte globulin (rATG) and then with sirolimus and tacrolimus maintenance. After 1 year, about 40% of patients were insulin independent with 100% demonstrating graft function as measured by circulating C-Peptide values greater than 0.3 ng/mL. After 2 years, the median exogenous insulin requirement was zero with the highest doses still remaining less than 10 IU/day. Compared to the Edmonton Protocol, which did not demonstrate this level of success, CIT-07 differed by several peritransplant procedures [22]. This included a short period of islet culture, early initiation of rATG, and modulation of anti-inflammatory therapy to mitigate instant blood-mediated inflammatory reaction (IBMIR) with a combined insulin and heparin infusion followed by a week of additional low molecular weight heparin and intensive insulin therapy for 2 months. A cohort of 11 patients in the trial treated at the University of Pennsylvania demonstrated improvement of beta cell secretory capacity, and all showed complete insulin independence after a year [22].

Human islet allotransplants, when properly administered, cultured, and immunosuppressed, can clearly provide useful therapy for years. The caveat to this approach is the potential side effects of chronic immunosuppression including direct

toxicities and increased malignancy risks. Tacrolimus and other calcineurin inhibitors are associated with nephrotoxicity and beta cell toxicity [23]. Other side effects include peripheral edema, hypercholesterolemia, abdominal pain, headache, nausea, diarrhea, pain, constipation, hypertriglyceridemia, hypertension, fever, urinary tract infection, anemia, arthralgia, and thrombocytopenia [24]. While many of these side effects are not life-threatening, they present a significant burden of potential morbidity to the patient.

Islet Transplantation: Site Selection Considerations

In their native location, β -cells are contained within islets which are dispersed within the exocrine pancreas. The human pancreas contains approximately one million islets, each consisting of about 1500 cells but ranging from only a few cells to over 12,000 cells [25]. The majority of the venous drainage of the pancreas is via the pancreaticoduodenal veins into the portal vein. This supports the liver receiving higher levels of insulin than the rest of the body. Such portal insulin delivery supports liver glycogen synthesis and suppression of endogenous glucose production [26]. Ideally, an islet replacement strategy would recapitulate this physiology, but portal insulin delivery is not required to achieve normoglycemia. Evidence for this comes from whole organ pancreas transplants, where venous drainage is most often into the systemic circulation via the recipient's vena cava or an external iliac vessel and less frequently into the portal circulation via the superior mesenteric vein. While fasting insulin is significantly lower with portal drainage, no difference has been found in comparing portal versus systemic drainage with regard to fasting and stimulated glucose or hemoglobin A1c [27].

Within the pancreas, islets are richly vascularized by direct arteriolar blood flow. Microsphere flow studies in animals demonstrate that islets, which make up only about 1–2% of the mass of the pancreas, receive greater than 10% of the pancreatic blood flow [28]. This high degree of arteriolar blood flow is likely important for rapid nutrient sensing from the blood. Indeed, mice with decreased vascularization of the islets due to β -cell-reduced VEGF-A expression have impaired stimulated insulin secretion that has been shown to be related to these vascular alterations and not β -cell dysfunction [29].

The portal vein is currently the most common transplant site for islets. Pancreatic islets infused into the portal vein lodge in distal tributaries. These islets are revascularized by branches of the hepatic artery [30]. In an animal model, glucose and arginine administered through the hepatic artery, but not through the portal vein, induced insulin release from intraportally implanted islets [31]. Unfortunately, this intraportal site has generally had low revascularization of islets [32]. Other transplant sites that are being explored include muscle, pre-vascularized subcutis, and omentum. Of these, the omental pouch appears to have the best glucose kinetics with naked islets [33, 34]. However, with appropriate vascularization, as seen in whole organ pancreas transplant, there are likely many suitable sites.

Encapsulating Islets: Biomass Considerations

Encapsulated β -cell therapy has not yet demonstrated the level of success of naked islets, but remains a very active area of R&D in the pursuit of a therapy that obviates the need for chronic immunosuppression. In theory, encapsulating materials can be designed to support the flux of therapeutic molecules, oxygen, and nutrients while creating a permselective barrier against harmful elements of the immune system. But these ideal transport properties are difficult to achieve in the dynamic environment of the host in a way that is predictable *in vitro*, owing to interaction with host proteins, and involvement of the immune system against either materials or cell debris. Rather, several encapsulation systems have been fabricated out of membranes with much larger pore structures that allow some elements of the immune system to pass, favoring transport of the necessary nutritive elements at the expense of potentially injurious immune molecules or inflammatory cytokines. The sections below highlight some of the challenges of encapsulation system design, both in the context of primary islets and stem cell-derived islet-like tissue.

In the endocrine pancreas, islets are organized around a rich network of capillaries with about ten times more fenestrae than the exocrine tissue that surrounds them [35]. In this arrangement, β -cells are typically distanced by a single cell from the bloodstream [36], allowing efficient sensing of glucose and secretion of insulin with minimal diffusive resistance, as well as enhanced oxygenation and nutrient transport. There is also data suggesting that the presence of endothelial cells and their secreted growth factors is necessary for β -cell function. In several animal models, deletion of VEGF-A is associated with glucose intolerance [37, 38].

Fully contained cell encapsulation systems necessarily separate islets or β -cells from the bloodstream, relying instead on diffusive or assisted transport of key solutes through the biomaterial and encapsulated (and avascular) biomass. For a human dose of islets, the distance that insulin must travel is quite far. At a dose of 800,000 IEQ as evaluated in the Edmonton Protocol and CIT-07, and a diameter of 150 μm for each IEQ, the dose would occupy a packed volume of about 1.4 cc of solid tissue. Considering that the abdominal cavity of an adult could probably comfortably house a 10-cm disc-sized encapsulation system, depending on location, the disc would need to be at least 176 μm thick to accommodate an internal volume of 1.4 cc, not including any of the materials used to make the device. Estimating membrane thickness at about 25 μm , this hypothetical encapsulation device would be 226 μm in total thickness with 100% packing density inside the device, e.g., the spherical islet clusters would be compressed into a solid tissue mass. The β -cells in the device core would be separated from the outside by 88 μm of biomass and 25 μm of biomaterial, for a total distance of 113 μm . This is 5–10 times the distance in the innate pancreas where β -cells are only separated by a one to two 12 μm cells. In addition to greater distance from an oxygen source, the diffusion of oxygen through solid tissue encased within a permselective membrane is significantly slower than diffusion through a liquid [39]. Further complicating matters is the limited vascularization that can be accommodated by the surface of indwelling abdominal implants,

which in simple formats cannot approach the relative density of vessels to β -cells in the pancreas [40].

Microencapsulated islets have the advantage of potentially uniform distribution throughout a cavity and, depending on size and configuration, a greater surface area to volume ratio (SA:V). Conformally coated islets have a barrier thickness of about 25 μm and SA:V of about 300 cm^{-1} and are administered as a suspension that can distribute throughout the peritoneal cavity or can be localized within an enclosed pocket in the renal subcapsular space, omentum, or epididymal fat pad [41]. In this configuration, the 800,000 cell clusters that make up a human dose can be delivered separately in that suspension, allowing the full surface area of the membrane to have contact with the host, with the diffusion distance dictated by the thickness of the barrier layer and surrounding tissue. In terms of surface area to volume, this encapsulation modality is about three times higher than the 10-cm disc described earlier. Conformally coated C57BL/6 islets were evaluated *in vitro* for insulin transport kinetics and were implanted into the renal subcapsular space to assess control of diabetes [41]. In dynamic perfusion experiments, no delay in insulin secretion was observed in coatings comprised of crosslinked poly(ethylene glycol) (PEG) and alginate in comparison to naked islets. Further, the duration of glucore sponsiveness was enhanced in culture, demonstrating a high stimulation index for multiple days. *In vivo*, the subcapsular coated syngeneic islets controlled glucose levels for 112 days, with little evidence of fibrosis or macrophage infiltration. These results highlight the significant advantage of maintaining a high SA:V ratio, which translates into more desirable insulin kinetics and the ability to transplant into environments such as the renal subcapsular space that would not be permitted with larger format microcapsules or macrodevices.

Traditional microcapsules of about 1 mm in diameter, with a thinner membrane wall and about three islets per capsule, have a twofold lower SA:V than the bilayer example device described earlier but with an even greater diffusion distance. But these capsules have other advantages, including rapid solute flux through a very hydrophilic membrane, high levels of biocompatibility, anti-fibrotic properties, and durability. Neither microcapsule system is completely retrievable, a significant pitfall in the case of an adverse event or complication. A comparison of conformally coated islets and microcapsules is shown in Fig. 2.1.

With these physical limitations relative to the innate pancreas, micro- and macroencapsulation platforms have evolved to address these and other failure modes through years of research. This sequence of potentially adverse events begins with issues during fabrication and filling, to acute implant responses that cause damage to encapsulation devices or the cells inside, to chronic failure involving the autocatalytic process evoked when cells within the device die, releasing antigens that are shed into the surround tissue provoking an immune attack, to ramifications of mechanical failure at the implant site. Some of the challenges facing cell encapsulation are shown in Fig. 2.2. This diagram attempts to depict the relative magnitude of some encapsulation failure modes, either process-related or that occur *in vivo*, as a series of peaks and valleys.

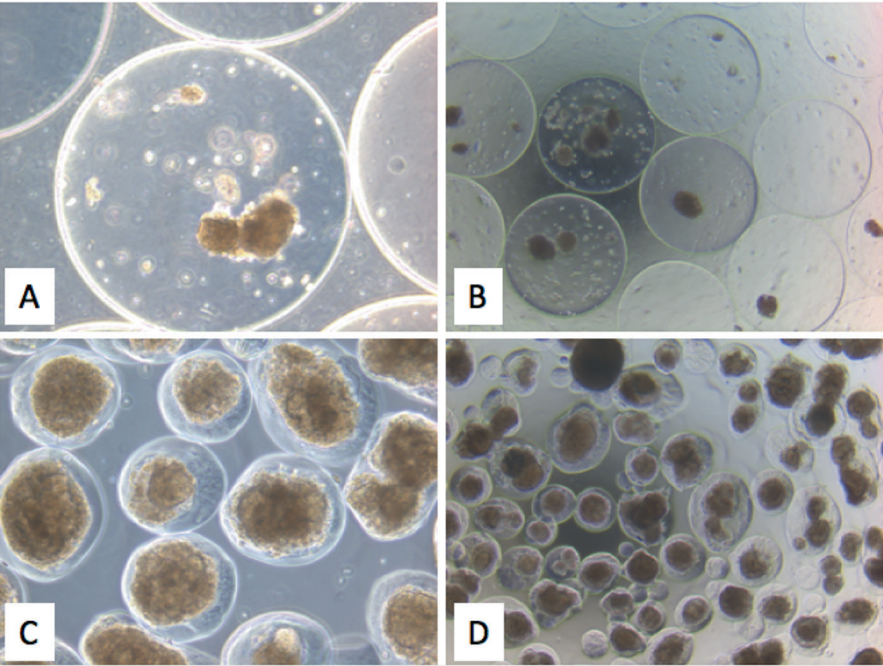


Fig. 2.1 Microencapsulated and conformally coated islets. (a) 10 \times and (b) 4 \times magnification of alginate-encapsulated islets. (c) 10 \times and (d) 4 \times magnification of PEG conformally coated islets (Image courtesy of Alice Tomei, Diabetes Research Institute)

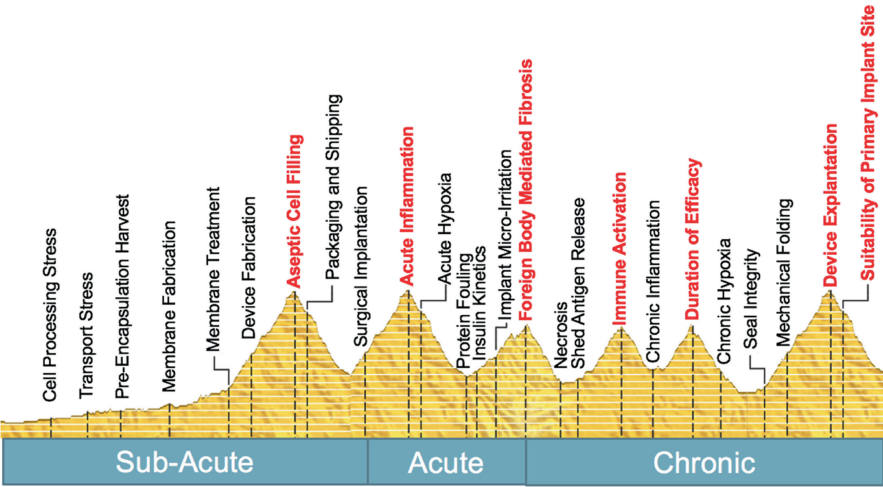


Fig. 2.2 Potential failure modes along the path to long-term device success. The x-axis represents time, and the height of the peaks represents a conceptual magnitude of the challenge

Islet Encapsulation Failure Modes

Subacute Processing Stress

Islets isolated from donor pancreata are subjected to an enormous amount of processing stress, due in large part to the variability in the enzyme blends [42], age and health status of the donor [43], and other islet-processing variables [44]. Once healthy and viable cells are achieved in culture, they must be harvested for encapsulation. This process involves concentration of the cell suspension used in culture such that it can be efficiently encapsulated, usually involving sedimentation, centrifugation, and a series of washes. During the encapsulation process, islets or cell suspensions can be adversely impacted by temperature, shear stress due to fluid path limitations, hypoxia, osmotic gradients, and stress associated with exposure to the encapsulation materials [45]. Post-encapsulation storage and transport conditions mark the final hurdles prior to implantation.

Acute Implant Failure

After implantation, encapsulation devices are exposed to a site of injury created by the incision, through blunt dissection and trauma to the surrounding tissues, potentially by anchoring sutures, and a transition from media with defined content to the physiologic environment. Some level of acute inflammation will undoubtedly accompany implantation, as proteins are adsorbed onto the biomaterial surface leading to varying activation of the coagulation cascade and complement system [46]. Fibrin deposition and platelet activation prime polymorphonuclear cells to attach to the surface via integrin receptors [47], secreting proteolytic enzymes and reactive oxygen species (ROS), followed by IL-8. As IL-8 secretion is decreased, migration of monocytes and macrophages leads to activation and potentially foreign body giant cell formation [48].

Macrophage polarization is an important component of the inflammatory response that can be impacted by the size, shape, and chemistry of the biomaterial [49]. M1 or classically activated pro-inflammatory macrophages secrete toxic reactive oxygen and nitrogen intermediates and pro-inflammatory cytokines including IL-1 β , IL-6, and TNF- α . These cells are the inducer and effector cells in the Th1 type response. In contrast, M2 macrophages activated through the alternative pathway are involved in polarized Th2 reactions and are associated with pro-healing responses. In cutaneous wound healing, the early inflammatory stage of wound healing is dominated by expression of genes associated with M1 macrophages, while the later stages involving tissue remodeling and angiogenesis are associated with mostly M2 genes [50]. The plasticity of macrophages enables a transition between the two phenotypes that is required at a particular time and place in the wound healing response. Fibrosis associated with a protracted inflammatory response can result from dysregulation of macrophage phenotype transitioning.

The inflammatory response associated with implantation of biomaterials and regulated by macrophage phenotype can be modulated by manipulation of chemical and physical material properties. Macroporous biomaterials with pores on the order of 30–40 μm have been associated with minimal fibrosis and high levels of vascularization [51], while non-porous versions of equivalent materials elicit a foreign body response and become encapsulated in fibrosis. In the myocardium of nude rats, acellular scaffolds composed of collagen-modified pHEMA-co-MAA hydrogels were evaluated for fibrous encapsulation and vascularization. In this study, the ratio of M2/M1 macrophages was significantly higher in the group with the highest porosity, with reduced fibrotic response and increased density of neovascularization [52]. In nanofibrous electrospun fiber scaffolds, filament diameter and orientation have also been shown to modulate acute inflammation, with a reduction in foreign body giant cells compared to a film of the same material composition [53]. Similarly, an M2 macrophage phenotype was associated with large or widely separated features on PVDF surface, as the expression of CD163 was significantly enhanced in the presence of a microtextured surface in comparison to a smooth control [54].

The mechanism and extent of inflammation can impact encapsulated cell systems by secreting the so-called cytokine storm, a set of inflammatory cytokines, as well as reactive oxygen species (ROS) such as superoxide, nitric oxide, hydrogen peroxide, and hydroxyl radical that induce oxidative damage [55]. One strategy to prevent oxidative damage is to incorporate a superoxide dismutase (SOD) mimetic into the polymer structure of the immunoisulatory barrier, which can provide protection against ROS injury as an antioxidant [56]. In this work, β -cells incubated in soluble Mn(III) tetrakis[1-(3-acryloxy-propyl)-4-pyridyl] porphyrin, an SOD mimetic, and superoxide was generated by adding xanthine and xanthine oxidase. Based on alamar blue staining, metabolic activity was shown to be increased about fourfold in the presence of the SOD mimetic. Poly(ethylene glycol) diacrylate (PEGDA) was also used to encapsulate MIN-6 cells together with the SOD mimetic, crosslinking with a photoinitiator and 365 nm light. Incorporated at a concentration of 100 μM , the mimetic provided protection against 25, 50, and 100 μM xanthine in a dose-dependent fashion.

A unique approach to counteracting the cytokine cascade is to co-encapsulate an immunomodulatory chemokine together with islets [57]. CXCL12, a CXCR4-binding chemokine, has demonstrated anti-inflammatory suppression of effector T cells in sites of injury. Murine islets incubated in media containing CXCL12 were implanted under the kidney capsule of C57BL/6 mice. The PBS control and 100 ng/mL CXCL12 group showed control of diabetes for only a couple of weeks, while mice implanted with 1 $\mu\text{g/mL}$ CXCL12 were controlled for over a month. CD3+ cells within the graft were reduced by about fourfold in the high-dose CXCL12 group compared to the PBS control. Allo-sensitized NOD/LtJ mice were implanted with murine islets co-encapsulated with 1 $\mu\text{g/mL}$ CXCL12 in ultrapure, low-viscosity alginate high in mannuronic acid content. In comparison to the control group, which demonstrated normoglycemia for about 10 weeks, the group loaded with CXCL12 maintained glucose control for the duration of the experiment, 15

weeks. This was extended to a xenogeneic model wherein porcine islets were implanted into diabetic C57BL/6 mice, demonstrating glucose control for 300 days.

Chronic Failure of Cell Encapsulation Systems

If encapsulated cells are able to withstand the early stresses after implantation, and engraft or exist in a particular anatomical site without encountering destructive fibrosis, the timeline for therapeutic benefit becomes limited by the ability of the delivery system to sustain adequate diffusion and mechanical integrity for the lifespan of the cells. In the case of macrodevice membranes, this requires resistance to protein fouling such that diffusivity is maintained sufficient to support oxygen transport to the cells within. Mechanical integrity of macrodevices, including individual components as well as the seals that hold them together, is another important site of potential failure as the implant encounters physiologic conditions for months or years. Membrane coatings, sealants, and frames are all susceptible to material changes due to potential degradation, leaching of critical excipients, swelling, hydrolysis, or protein and cell deposition. Grossly, a change in the shape or topography of the implant can result in stimulation of an inflammatory event leading to a second wave of acute inflammation. Of particular concern to large-footprint macrodevices, especially those comprised of thin bilayer membrane sections with relatively little mechanical support, is the propensity for such devices to fold, crease, or contract. In surgical sites such as the subcutaneous space, this can be exacerbated by the micromotion-triggered inflammation that is inherent to regions of the body or tissues that incur the most movement [58].

The failure modes highlighted in this section make up a significant amount of the research focus in the field of cell encapsulation. The following sections will describe some of those efforts in the context of both micro- and macroencapsulation systems and whether there is any inherent advantage to using primary tissues compared to stem cell-derived or genetically modified cell lines.

Immune Rejection

Immunoprotective encapsulation systems are based on the premise that permselective membranes can limit or deny the passage of harmful elements of the host into the encapsulated microenvironment, while nutrients and oxygen flow freely. Depending on the size and shape of the solute of interest, their flux can be controlled by altering membrane parameters such as porosity and thickness, as well as the hydrophobicity of the surface, the radius and tortuosity of the pores, and by creating gradients within the membrane [59]. Membranes originally developed for other biological applications such as protein purification have been used in this capacity for decades and has led to the development of a number of materials with so-called immunoisulatory capacity.

Much has been written on the theory of immunoisolation as it applies to cell therapy devices, but many questions remain regarding the relative impact of cellular vs. humoral immune protection. A cellular immune response to live, encapsulated

cells is minimized due to the physical separation of encapsulated cells from the host immune system [60]. But the release of small components of dead or dying cells, or shed antigens, can stimulate such a response. A humoral immune response mediated by immunoglobulin and complement is another likely pathway for immune rejection, although there is some evidence that exclusion of the elements of the complement system is not an absolute requirement as they are inactivated during outward diffusion [61]. For an immunoprotective membrane that excludes antibodies and complement to provide utility in the treatment of T1D, it must allow the outward flux of insulin and cellular waste products and inward flux of glucose and oxygen. Insulin is a 5.8 kDa molecule with a Stokes radius of about 1.35 nm, while IgG is about 5.4 nm in diameter, and elements of the complement system are only slightly larger at about 13 nm [62, 63]. The ability to deliver insulin to the outside freely without diffusion of IgG to the inside requires a very narrow range in which pore size can be optimized.

Diffusion through a membrane by passive processes requires movement of the solute throughout the matrix as dictated by the physical constraints of the membrane (thickness, porosity, tortuosity), the concentration gradient, and the available surface area. Fick's law describes this relationship as shown below, where J = flux, ϵ m = porosity, C = concentration, D = diffusion coefficient, and τ = tortuosity. Solute flux can be viewed as the absolute performance of a membrane with a given set of characteristics and physical properties and is inherently tied to porosity and tortuosity.

$$J_{eff} = -\epsilon D_{eff} \nabla C = -\epsilon \frac{D_o}{\tau} \nabla C$$

Conceptually, a porous structure with pores smaller than 5.4 nm in diameter could provide an immunoisulatory interface. But rather than a monodisperse assembly of transmembrane pores, most membranes contain a range of pore sizes with varying interconnectivity and tortuosity that together govern solute transport. These membranes include materials produced by phase inversion, controlled stretching, and sintering [59]. Phase inversion produces primarily anisotropic membranes from materials like polysulfone, polyethersulfone, cellulose, and others. As a diffusive barrier, such membranes typically achieve permselectivity within a thin region or limiting skin, surrounded by a less dense region that serves as a protective layer (Fig. 2.3). Together, these membrane layers achieve a very high level of porosity, in some cases up to 80%, but usually with very high tortuosity. Controlled stretching, sintering, and electrospinning [64] also produce potentially immunoprotective membranes that are more uniform in character with minimal pore gradients. These structures can also have extremely high porosities but are inherently very tortuous.

The relationship between porous tortuosity and absolute porosity may be the most impactful on defining immunologically relevant molecular weight cutoffs. While the spinning chemistries described above produce a range of pore sizes and pore gradients, other techniques can create a discrete pore size with very minimal tortuosity. Track etching is a process that produces almost perfect cylindrical pores

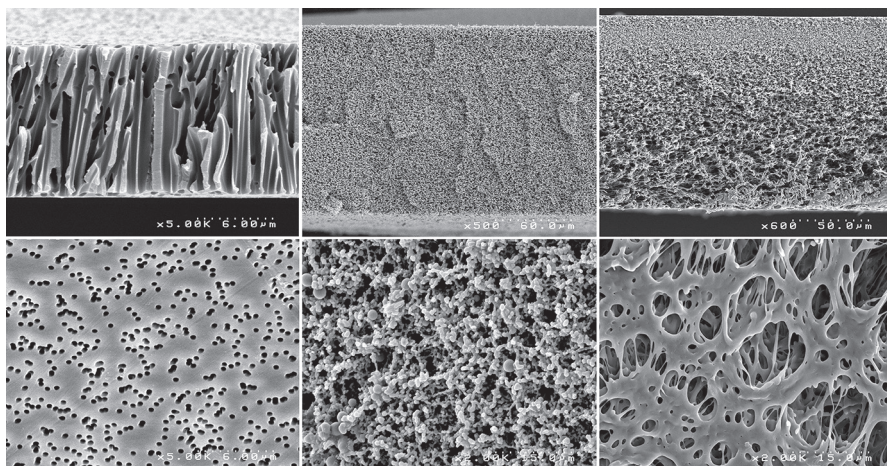


Fig. 2.3 Scanning electron micrographs of membrane materials. (*Left*) *Top*, membrane wall of a track-etched polycarbonate membrane; *bottom*, surface of the same membrane. (*Middle*) *Top*, membrane wall of a commercially available polyvinylidene difluoride membrane; *bottom*, surface view of same membrane. (*Right*) *top*, wall of a poly(ether sulfone) membrane; *bottom*, surface of the same membrane

using a technique developed by GE in the 1960s [65]. The process bombards a polymer thin film, typically polycarbonate or PET, with a collimated beam of high-energy nuclear particles resulting in tracks that are later opened by a heated peroxide or NaOH solution. This type of membrane is theoretically well suited for immunoprotection, as a truly uniform pore distribution [66] can be achieved within a relevant pore size range. The caveat to this approach is that porosity is limited due to the inability to create tracks at very high density without loss of mechanical integrity, with a maximum of about 20–40% depending on pore size, thereby decreasing the resulting flux of the membrane. Similarly, inorganic membranes have been produced with low-tortuosity nanopores from silicon [67], aluminum/aluminum oxide, and titanium/titanium oxide [67]. While these membranes offer an exceptionally narrow pore distribution, less than 5% in some cases [68], at a very minimal thickness, they have varying degrees of biocompatibility that confound their utility. Nanoporous polycaprolactone, a very slowly biodegradable membrane, has been engineered using zinc oxide nanorod assembly to produce pores in the range of 30–100 nm [69]. These membranes would not completely restrict passage of a 5.4 nm IgG molecule, but they are extremely biocompatible, flexible, and could theoretically be produced with much smaller pore sizes. However, the porosity of these membranes is not described and would play an important role in determining diffusive behavior. Membrane coatings have also been used to restrict the diffusion of membranes with large pore size. Expanded polytetrafluoroethylene (ePTFE) membranes with nominal pore size of 400 nm were evaluated for the ability to pass IgG or C1q [70]. When impregnated with ultrapure alginate high in mannuronic acid content and then crosslinked with barium chloride, the diffusion of IgG and

Clq was reduced to 0.5% after 20 h of incubation, while the diffusion coefficient of insulin only decreased from $2.38 \times 10^{-7} \text{ cm}^2/\text{s}$ in the untreated membrane to $1.11 \times 10^{-7} \text{ cm}^2/\text{s}$ for the alginate-impregnated membrane.

Alginate as a microencapsulation system has also demonstrated permselective properties depending on the type of alginate employed, the crosslinking agent, and whether or not there is an intermediate polycation [71]. Alginate capsules made by the traditional A-P-A process (alginate-polycation-alginate) were compared to alginate capsules that were simply crosslinked with barium chloride and left as solid hydrogel spheres [72]. In this study, encapsulated rat islets were transplanted into the peritoneal cavity of diabetic rats and evaluated for glycemic control over the course of months in comparison to renal subcapsular implants. In both cases, the encapsulated allogeneic transplants corrected diabetes more quickly than the unencapsulated control. However, both capsule formulations were associated with kinetic delays *in vitro* and *in vivo* suggesting that significant diffusion limitations prevented adequate transport. Alginate high in mannuronic residues is also associated with greater diffusivity than capsules made from alginate containing primarily guluronic acid due to the reduction in available crosslinking sites present in G-blocks [73]. In an experiment comparing APA capsules fabricated using the same polyornithine intermediate layer and the same crosslinking agents, only the base alginate material was varied by selecting a high-M Keltone alginate or a high-G Novamatrix alginate. The release of a 20 kDa FITC-dextran marker was about only 8% higher in the high-M group than the high-G group, and the molecular weight cutoff values were very similar at 165 kDa for the high-M group and 156 kDa for the high-G group. This illustrates that in the presence of a polycation, the diffusive control of the capsule formulation is dominated by the ability of the polycation to intercalate within the inner and outer layers of alginate. In comparison to alginate slabs crosslinked with only calcium, the diffusion coefficient of bovine serum albumen was several log orders of magnitude faster ($2 \times 10^{-6} \text{ cm}^2/\text{s}$ vs. $1 \times 10^{-10} \text{ cm}^2/\text{s}$).

Hypoxia

Pancreatic islets are organized in a trilaminar structure with vessels that circulate along both of its sides, providing access to oxygen within a distance of 2–3 cells for any given β -cell within the islet [74]. This translates into higher oxygen exposure for β -cells in comparison to other cell types in the body during development and in the adult pancreas. As a result, β -cells are extremely reliant on oxygen for function. The transition from the intact pancreas to isolated islets involves significant stress and disruption of the organization that is present when residing in the pancreas. All functional vascular supply is lost, and the impact on islet structure is primarily one of diffusion constraints, as the diffusion distance to the cells in the core increases from about 2–3 cells to about 15 cells. Hypoxic centers can be visualized in isolated islets in culture within a matter of days [39], and in the context of encapsulation systems, diffusion distances and consumptive demand are increased significantly. As described previously, about a cubic centimeter of solid tissue is required for human therapy. To organize such a tissue mass in a way that circumvents both diffusion limitations and the consumptive load of the β -cell mass, e.g., the cumulative

amount of oxygen that is consumed in relation to the amount of oxygen that is present requires a reduction in the packing density, thickness, and the materials in the encapsulation system must not inhibit transport of oxygen.

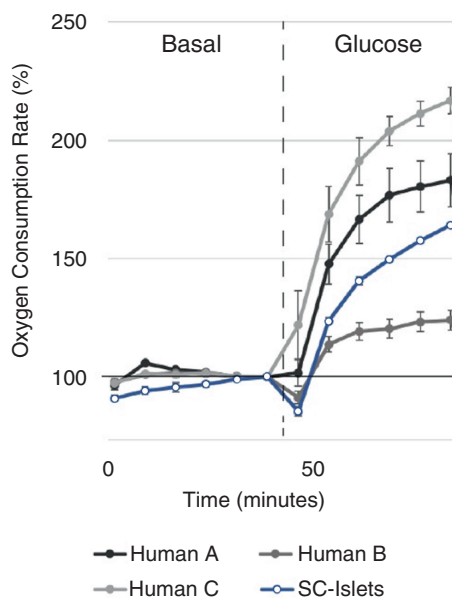
The threshold for islet hypoxia may be much lower than for glucose-stimulated insulin secretion, indicating that islets could potentially be transplanted and remain viable without providing function. This oxygen concentration threshold may be as low as 10 mmHg for function and 0.1–0.44 mmHg for viability [75, 76]. In vitro, second-phase insulin secretion was reduced at only 60 mmHg, and the total secretion rate was reduced by 50% at 27 mmHg [77]. In a human islet with about 1560 cells and a diameter of about 150 μm [78], the outer surface would need a pO_2 of about 35–40 mmHg to keep even the innermost cells alive and about 45–50 mmHg to keep those same cells functional [75].

The partial pressure of oxygen in the transplant site can be variable depending on the disease state, the anatomical location, and the extent of injury incurred during the implantation process. In mice maintained under normal ambient conditions with 20% oxygen, tissue oxygen partial pressure varied from about 50 mmHg in fat, 26 mmHg in muscle, 27 mmHg in liver, 25 mmHg in kidney, and 42 mmHg in the subcutaneous space [79]. The oxygen partial pressure of the peritoneal cavity is about 40 mmHg. Given the published threshold for an islet to function of about 45–50 mmHg, and the increased diffusion distance and decreased diffusivity when on the other side of a permselective membrane, none of these transplant sites would seemingly be able to support a biomass of any significant size without a supplemental oxygenation strategy.

The oxygen that diffuses into encapsulation devices is quickly consumed by the viable biomass that remains. As β -cells consume more oxygen than most other cell types including tumor cells [80], the consumptive load of encapsulated islets is compounded by the absolute number of cells required, presenting a serious obstacle to longevity. The oxygen consumption rate (OCR) of human islets has been characterized extensively and has recently been retrospectively correlated with clinical trial outcomes [81]. In patients with severe pancreatitis that received total pancreatectomy and intraportal autotransplantation, dosing by total islet equivalents (IE dose) was compared to dosing by viable islet equivalents as inferred by measuring oxygen consumption rate (OCR dose). In this analysis, both metrics correlated well with insulin independence and OCR doses greater than 150 $\text{nmol O}_2/\text{min}\cdot\text{mg DNA}$ supported previous studies in mice suggestive of a functional dose threshold [82, 83].

Resting islets consume less oxygen than islets stimulated with glucose, which triggers ATP-dependent insulin secretion and significantly higher mitochondrial respiration [84]. Rat islets exposed to 3 mM glucose followed by 20 mM glucose showed a roughly sixfold increase in OCR upon glucose stimulation, increasing to about 0.25 $\text{nmol}/\text{min}/100$ islets. Similarly, nonhuman primate islets were evaluated in microplate-based assay (BD Biosciences) using an oxygen-sensitive fluorescent dye. Compared to a basal OCR of about 2.7×10^4 fmol/min , glucose-stimulated

Fig. 2.4 Oxygen consumption rate (OCR) of human or stem cell-derived islets as a function of glucose stimulus. *Y*-axis represents OCR values normalized by basal levels (Image courtesy of Semma Therapeutics)



NHP islets increased to about 1.1×10^5 fmol/min in 16.7 mM glucose. In the same study, the group established that human islets secreted insulin at a similar magnitude as they consumed oxygen. In 5.6, 16.7, and 33.3 mM glucose solutions, OCR increased from about 2.5×10^4 to 5×10^4 to 5.8×10^4 fmol/min/100 IEQ. Accordingly, insulin secretion increased from about 600 to 900 to 1000 ng/mL/100 IEQ. A linear correlation was calculated with $P < 0.01$, highlighting the critical dependence of insulin secretion on oxygen consumption.

Human islets as well as stem cell-derived islets show similar behavior as demonstrated by the Seahorse extracellular flux technique (Fig. 2.4). Here, cells are exposed to 2.8 mM glucose for roughly 40 min and then the solutions are spiked to 20 mM glucose, leading to a 50–220% increase in OCR values. Three separate human preparations are shown to highlight the inherent variability of primary cell preparations. The interdependence of insulin secretion on oxygen consumption illustrates the importance of oxygen supply in encapsulation systems. While a viable cell may consume 150 nmol O_2 /min*mg DNA, a functioning cell consumes 300 nmol O_2 /min*mg DNA under peak load. As an encapsulated biomass of about 800,000 islets as in the CIT-07 trial, or about a billion cells (roughly 6.6 mg DNA based on 6.6 pg per diploid cell [85]), the graft would need about 2 μ mol/min to support insulin secretion. In comparison, 1 mL of peritoneal fluid at an oxygen partial pressure of 40 mmHg only contains about 0.056 μ mol oxygen or roughly 3% of the amount needed to support this function for a single minute.

Strategies for Addressing Hypoxia

Refillable Gas Supply

Because of this serious oxygen limitation, several strategies are in development to support encapsulated cells with oxygen from an external source. Beta-O₂ has developed a macrodevice built around a central oxygen chamber wherein patients can replenish the device's oxygen supply percutaneously by injecting oxygen daily into a small port [80]. The islets are contained within an alginate matrix 600 μm in depth at the surface of the device, separated from the internal oxygen chamber by a silicone rubber membrane (Fig. 2.5) that provides a gas permeable barrier between the central cavity and the cell chambers that flank it. This creates a gradient of oxygen concentration to develop from the supply (95% oxygen) to the cell chamber (~77%). The device offers immunoprotection by incorporating an ePTFE membrane with 400 nm pores that are impregnated with a highly crosslinked high-M alginate, resulting in significant reduction of IgG and complement diffusion [70].

The device is designed for hyperoxic conditions (<550 Torr) to support packing densities as high as 3600 IEQ/cm², or 11% V/V, and has progressed through rodent prototypes to pig and human sizes [80]. The device design process made extensive use of mathematical modeling, both for evaluating the geometric requirements of the cell cavity and the pressure and concentration of the supplied oxygen gas. The result was that a 95% oxygen mixture could be administered into the chamber at a pressure of 1000 Torr, but the multi-chamber design of the device, separated by silicone membranes, maintained the critical pO₂ of less than 550 Torr and greater than 100 Torr. In studies using rat islets implanted into diabetic Sinclair pigs, glucose levels were controlled for 75 days with an initial dose of about 6700 IEQ/kg. But as these pigs grew quickly, glycemic control was lost when weight gain was sufficient to bring the dose below 4000 IEQ/kg [70]. A similar sized device was also evaluated

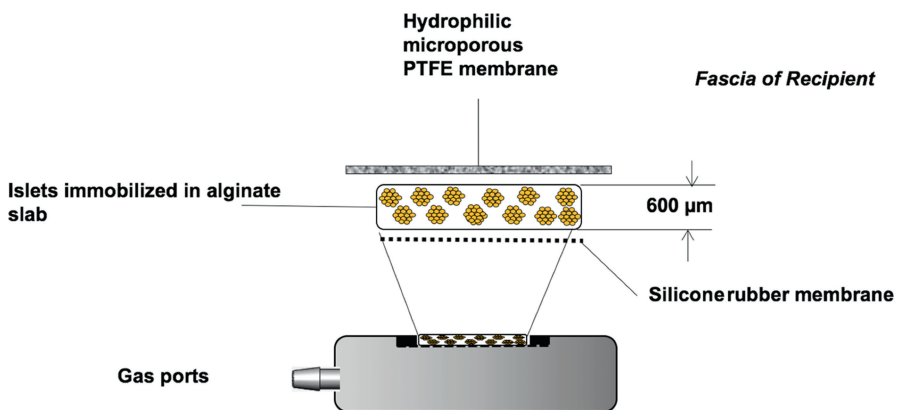


Fig. 2.5 β -Air oxygenated macroencapsulation device developed by Beta-O₂ (Image courtesy of Avi Rotem, Beta-O₂)

in human clinical trials using a sub-therapeutic dose of human islets (2100 IEQ/kg). After 10 months, this marginal mass resulted in a reduction of exogenous insulin requirements of 15% and a reduction in HbA1c from 7.4% to 6.4%. [86]. The device is currently in clinical evaluation in a pilot trial (NCT02064309), and a next-generation device is in development that requires less frequent oxygen refilling and that has a larger cell capacity [87].

Artificial Oxygen Carriers

The use of artificial oxygen carriers (AOCs) in microencapsulation systems has been explored as a means of improving the diffusion of oxygen in alginate systems. AOCs bind, transport, and release oxygen into the target site. Perfluorocarbons have been studied in this role since the 1960s but their toxicity profile includes prolonged presence in the reticuloendothelial system and is associated with chemical pneumonitis [88]. Perfluorocarbon products have been approved by the FDA but their use was discontinued in 1994 [89]. Still, AOCs represent a chemical means by which an oxygenation solution could be incorporated into encapsulation devices. Perfluorocarbon (PFC) AOCs have been evaluated as a 400 nm emulsion making up 36% V/V of an alginate capsule formulation crosslinked with barium [90]. In these studies, capsules containing 2.4×10^7 cells/mL were prepared in alginate and compared to naked islets and alginate PFC microcapsules. The diffusion coefficient of oxygen in individual and combined systems was calculated, highlighting that PFC increased diffusion from 2.77×10^{-6} cm²/s for 2% V/V alginate to 9.36×10^{-6} cm²/s in a 70% emulsion with PFC. After 2 days in culture in low oxygen (3%), tissue recovery in the PFC formulation was significantly lower than in the alginate capsule control. OCR recovery showed no difference with or without the incorporation of PFC. Indeed in this study, histology revealed that there was minor toxicity of the PFC component to the islets.

Rather than using an emulsion, PFC has also been grafted directly onto alginate using a PEG-amide linker [91]. Alginate beads were made at 1.6% W/V and cross-linked with barium, but the gelation process was inhibited at higher PFC levels. Oxygen diffusion was increased in the PFC-grafted alginate by about 10% with a PFC loading of 0.05% W/V, demonstrating its potential in this application. Encapsulation of MIN-6 cells showed that the material had a high level of biocompatibility, with increases in cell number by MTT assay compared to the alginate control after a week.

Oxygen-generating materials have recently been evaluated as a means of introducing oxygen into the internal volume of encapsulation systems. These materials can be particularly useful in device strategies that rely on vascularization to support the oxygen demands of the encapsulated cells. As the vascularization process can take days or weeks to reach steady state, the encapsulated biomass must survive hypoxic conditions for at least some period of time, almost certainly in conditions that are not ideal for function. Oxygen-generating materials provide a potential short-term oxygen supply to overcome the immediate posttransplant period wherein

hypoxia is most extreme. Calcium peroxide (CP) has been used in this role as it can readily dissociate into oxygen and calcium hydroxide with the introduction of water [92]. One unique approach is to incorporate CP particulate into a polymer solution prior to casting of a membrane or cell scaffold. Scaffolds comprised of CP impregnated in polycaprolactone were fabricated by an electrospinning process [93]. In this work, scaffolds were generated with up to 10% CP which demonstrated antimicrobial activity in cultures of gram-negative and gram-positive bacteria. Osteoclasts cultured on these fibers, however, showed some evidence of cytotoxicity. CP was also incorporated into poly(D,L-lactide-co-glycolide) (PLGA) scaffolds designed to release oxygen for up to 10 days [94], a critical timepoint in the immediate post-implant period prior to engraftment. The PLGA-CP scaffolds were produced to be highly porous by incorporating paraffin particles, followed by removal in hexane. Scaffolds measuring 10 mm × 4 mm were maintained in hypoxic conditions at 1% oxygen, and generated oxygen was measured over 10 days in media supernatant, which maintained slightly higher oxygen levels than the scaffold controls (roughly 6 mmHg vs. 7 mmHg). NIH 3T3 fibroblasts seeded onto the scaffolds showed markedly improved survival after 2 weeks in culture in comparison to unmodified PLGA scaffolds. CP has recently been evaluated in an islet scaffold fabricated from porous PDMS [95]. In this work, the use of a very hydrophobic PDMS matrix was hypothesized to reduce the rate at which CP was converted to oxygen. The study showed that over 3–4 weeks of oxygen generation above 0.05 mol/m³ was possible, and in culture with MIN6 cells, PDMS-CP scaffolds rescued metabolic function in hypoxic conditions of 0.01 mM oxygen for 24 h. To demonstrate long-term utility, MIN6 cells were cultured for 3 weeks with or without PDMS-CP scaffolds. Both metabolic activity and recovered DNA were significantly higher in the group containing CP, indicating that oxygen generation by this method was supportive and nontoxic. Finally, MIN6 viability in both normoxic and hypoxic conditions was shown to be enhanced in the presence of CP at a cell loading of 250,000 cells per disc, whereas loading of 50,000 and 150,000 cells were associated with an equal or detrimental effect when compared to the PDMS controls, indicating a dose-dependency between the number of β -cells and the amount of CP.

Alginate microcapsules containing CP or sodium percarbonate (SP) has been produced by doping alginate solutions with oxygen-generating particulates [96]. SP particulates with average diameter of 330 μ m and CP particles with average diameter of about 3 μ m were incorporated into alginate solutions at a loading of 10 mg/mL with an islet loading of 5000 IEQ/mL. The droplet formation and coating processes were carried out at 4 °C to avoid premature degradation of SP particulates. Since alginate is readily crosslinked with divalent cations, calcium liberated during the dissolution of CP can accelerate gelation kinetics. The authors state that both of these formulations protect encapsulated islets from hypoxic conditions and reduce damage from oxidative stress.

Another strategy for oxygenated cell delivery is based on a core-shell microparticle containing peroxide in the core and catalase, an enzyme that catalyzes the decomposition of hydrogen peroxide to water and oxygen, within the outer shell [97]. In vitro, oxygen was generated by the 3.5 μ m microparticles at a concentration

of 1 mg/mL for about 12 days before reaching the level of the PBS control at day 14 (0.83–0.06 mg/L O_2). In hypoxic conditions, MIN6 cells cultured with the peroxide/catalase microparticles showed a statistically significant decrease in the presence of lactate dehydrogenase in the culture medium, indicating that the cells maintained higher levels of viability than the microparticle-free control. Additionally, cultures with microparticles showed no evidence of HIF-1 α translocation to the nucleus in comparison to controls. In VEGF-containing collagen scaffolds, rat islets co-loaded with oxygen-generating particles showed improved function for 30 days in comparison to naked islets and other combination matrices in alloxan-induced mice.

These temporary oxygenation strategies have merit in device designs that rely on vascularization for chronic oxygen supply to encapsulated islets. The device design and vascularization strategy can have a tremendous impact on the rate at which functional vascularization becomes available to support the cells, but incorporating a bridging strategy using the techniques described may provide a higher level of viability once a vascular network is established. This critical post-operative period may be the decisive factor not only in determining the functional capacity of the device but also by avoiding acute hypoxia-related cell death; there is additional benefit in mitigating shed antigen release and a potentially catastrophic immune response against the device. The next section will highlight several vascularization strategies that have been used to promote angiogenic support both for oxygen supply and as an interface for glucose sensing and insulin diffusion.

Vascularization

Bringing vessels from the host to the surface or around a device is an oxygenation strategy that does not necessarily require additional biologic molecules and that provides the added benefit of more direct access to the blood supply for glucose sensing and insulin secretion. The same kinetics that govern the diffusion of oxygen from hemoglobin within capillary red blood cells to tissue parenchyma would be applicable to capillary or arteriolar networks that form within or around devices. This exchange occurs between any two regions in which a P_{O_2} difference exists [98]. If the device is vascularized with functional arterioles, oxygen transport proceeds in a convective manner defined by the concentration of oxygen in the arteriole as shown in the equation below, where R = radius, v = velocity, and S = saturation.

$$Q_{O_2} = \pi R^2 v S_{O_2} [Hb] C_{Hb}$$

Capillary exchange of oxygen follows diffusive kinetics as governed by Fick's first law:

$$\frac{\Delta N}{\Delta t} = DA \Delta (\alpha P_{O_2}) / \Delta x$$

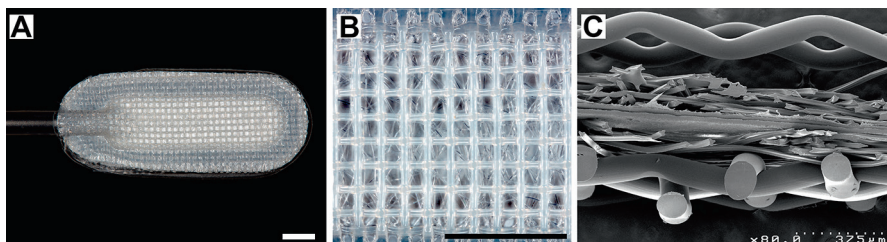


Fig. 2.6 (a) Low magnification and (b) high magnification of a rodent Theracyte device. Both **a** and **b** have scale bars that are equivalent to 2 mm in length. (c) Cross-section of a Theracyte device showing the outer polyester mesh, separated by small filaments from the inner ePTFE membranes

In diffusive transport, the extent of vascularization of the device and the density of capillaries within the vascularized tissue can impact kinetics by increasing the area (A) and distance (x) for diffusion [99].

One of the most thoroughly studied macrodevices, the Theracyte device, employs this strategy by incorporating multiple layers of engrafting material that stimulate ingrowth and vascularization [100]. The layered device is shown in Fig. 2.6 and comprises an outer polyester mesh, a smaller filament polyester mesh, an ePTFE membrane with internodal distance of $5\ \mu\text{m}$, and an interior $0.4\ \mu\text{m}$ ePTFE membrane. The assembly is sealed by ultrasonic welding and connected to a rigid polyethylene port for loading cells. Early in development of the Theracyte, a number of membrane candidates were evaluated in the rat subcutaneous space for the presence of a foreign body reaction and vascularization. The materials that were evaluated included a number of cellulosic membranes with pore size ranging from 0.8 to $8.0\ \mu\text{m}$, as well as polyester and ePTFE materials. Notably, $10\ \mu\text{m}$ nylon membranes and $1\text{--}12\ \mu\text{m}$ polycarbonate membranes were not associated with the formation of new vessels in proximity to the test materials. The group hypothesized that the large features of the nonvascularizing membranes enables cells from the host to attach and flatten out, leading to a classic foreign body response. In comparison, vascularizing membranes were thought to allow the cells to exist in a rounded configuration resulting in the release of pro-angiogenic factors.

Since this early work, the Theracyte device has been evaluated in a variety of cell encapsulation studies and has advanced through clinical design in several efforts to treat type 1 diabetes. To evaluate the transport properties of the device over the course of an implantation period, Theracyte devices were loaded with insulin and implanted in the subcutaneous space of rats. Using microdialysis sampling, the device was confirmed to deliver an equivalent dose to a subcutaneous injection, indicating that the membranes used in the device did not negatively impact insulin transport. The device was evaluated after 1, 2, 4, and 12 weeks following transplantation, demonstrating that as vascularization of the device progressed, the concentration of insulin in the serum was significantly higher in devices showing high vascular density within $15\ \mu\text{m}$ of the device [101]. Vascular density in this study was highest after 12 weeks. In the same model, the permeability of glucose was

measured in the device using the microdialysis technique in subcutaneously implanted rats [102]. These results also demonstrated that transport kinetics were retarded at all timepoints except for 12 weeks, which showed glucose concentration equivalent to the control animals. Finally, the group evaluated microcirculation around the device by introducing a laser Doppler probe through the loading port [103]. Flow was analyzed over the course of 3 months and was found to decrease significantly between day 1 and 4 weeks, from 158 to 72 perfusion units. This increased by 2 months to 138 PU and reached steady state after 3 months at 165 PU, again highlighting that the Theracyte device implanted subcutaneously may have relatively poor transport kinetics within the first months after implantation.

Based on these findings, several groups have explored the possibility of prevascularizing a device or a transplant site prior to introduction of the cells. This would allow for a transplant environment that is higher in oxygen supply and that would permit diffusion more freely at the time the cells are implanted into the host. Preimplantation of the Theracyte device was evaluated in Sprague-Dawley rats for 3 months prior to introduction of allogeneic islets [104]. Subcutaneous devices were accessed and filled with 1500 rat islets via the device port after 3 months, and filled devices were implanted contralaterally to serve as a prevascularization control. Devices explanted after 2 weeks revealed that preimplantation was associated with a 40% reduction in the amount of fibrotic tissue contained in the device with almost twice as many insulin-positive β -cells. Similarly, cure rates of preimplanted Theracyte devices in diabetic athymic mice were significantly higher than devices that were freshly implanted, with 100% of preimplanted animals reaching euglycemia compared to only 17% in the group implanted with preloaded devices [105].

Syngeneic pancreatic islets were implanted into a non-immunoprotective, prevascularized chamber device that was allowed to reside in the subcutaneous space for 40 days [106]. The device is comprised of a stainless steel mesh that is filled with a PTFE insert that can be removed after sufficient ingrowth occurs. The plunger was removed, and 3000 syngeneic rat islets were administered in saline solution, followed by closure of the device with a threaded PTFE seal. Seven out of the eight recipients achieved diabetes reversal within 6 days, in comparison to a cohort infused via the portal vein which showed reversal after 1 day. Both treatment groups demonstrated efficacy for 160 days. A comparison of insulin kinetics was conducted after 160 days by performing an intravenous glucose tolerance test. In this evaluation, islets contained in the device were about 30 min slower than islets in the liver to reach blood glucose levels less than 200 mg/dL.

Another approach that does not involve an indwelling device is to create a potential space, or “device-less” site that can act as a vascularized bed for cell or device implantation [34, 107, 108]. One iteration of this strategy involves implantation of a vascular catheter 4 weeks prior to transplantation, creating a vascularizing lumen into which islets are injected. In C57BL/6 mice induced with streptozotocin, a marginal mass of 150 syngeneic islets with 90% purity was implanted under the kidney capsule, in an unmodified subcutaneous space, or in the device-less site. Islets transplanted under the kidney capsule yielded euglycemia after about 18 days (94%), while the group implanted into the device-less site corrected glucose by day 34

(72%). Despite the delay, the grafts showed similar efficacy in glucose correction until they were removed after 100 days. Transplants into the unmodified subcutaneous site were not successful at correcting hyperglycemia. This approach certainly shows a potential benefit for naked cell injection and may be amenable to implantation of micro- or macroencapsulation modalities within a pre-vascularized site to improve acute oxygenation and transport properties.

Strategies for Mitigating Chronic Fibrosis

Coatings and Covalent Modifications

The foreign body response to biomaterials is an encapsulation failure mode that can, on its own, lead to a nearly impermeable, avascular granulomatous sheath surrounding the diffusive surface of devices effectively sealing it off from the host [109]. In a more moderate context, the biomaterial selected for an encapsulation system can act as an adjuvant to sway a potentially steady-state engraftment into irrecoverable inflammation. While the previous section on vascularizing strategies seeks to bring host tissue into or around the device, the ramification of doing that could very well lead to terminal fibrosis. Theracyte devices loaded with cadaveric parathyroid tissue were evaluated in nonimmunosuppressed humans for up to 14 months [110]. In this study, a cohort of patients undergoing parathyroidectomy were re-implanted with their own autologous tissue in Theracyte devices, while other patients with chronic hypoparathyroidism were implanted with allogeneic parathyroid loaded into Theracyte devices. Autologous transplants contained 22% endocrine tissue after up to 14 months and 63% fibrosis and about 15% was completely necrotic. In comparison, the explanted volume of devices loaded with allogeneic cells was dominated by fibrosis after only 4 weeks, with endocrine tissue accounting for only 1%, 5%, and 23% by volume. In all cases, there was no detectable increase in parathyroid hormone (PTH) level, potentially due to marked fibroblast overgrowth resulting from inflammation or an immune response.

Both micro- and macroencapsulation systems are susceptible to fibrotic encapsulation. A series of different sized spherical materials composed of hydrogels, metals, glass, and polymers was evaluated in C57BL/6 mice to evaluate biomaterial-specific foreign body responses. All of the materials were very smooth with no surface features greater than 1 μm . In surface area-matched doses implanted in the peritoneal cavity for 14 days, it was observed that spheres of 500 μm in diameter produced a significantly higher fibrotic response, while 1-mm diameter materials were associated with only very thin, mild responses [111]. The phenomenon was not altered at very long timepoints, as alginate spheres composed of SLG20 displayed this size-dependent fibrosis after 6 months when comparing 0.3-mm diameter spheres, which were significantly fibrosed, to 1.5-mm spheres, which were relatively free of cellular attachment. This observation was extended to the ability of alginate-encapsulated rat islets to cure streptozotocin-induced diabetic mice, where the cure rate of 1.5-mm capsules was maintained at 100% for about 120 days,

compared to 0% at the same timepoint for 500 μm capsules. The size dependency of foreign body response observed in these studies has important ramifications for micro- and macrodevice designs, as the features integral to both (capsule diameter, mesh spacing) may be optimized by geometry alone.

A combinatorial library of molecules was evaluated in a similar manner attached to a low molecular weight, ultrapure high-G alginate [112]. The library was generated based on the presence of amines, alcohols, azides, and alkynes in candidate materials that were evaluated for feasibility based on gelation kinetics and acute inflammation. Of these candidates, 16 were formulated into barium-alginate microspheres with diameters of 300–350 μm , within the size range discussed previously for propensity toward a foreign body response. Compared to unmodified alginate microcapsules, which displayed significant deposition of macrophages and myofibroblasts, the alginates modified with triazole functionality showed little to no presence of an inflammatory response. After 14 days in the peritoneal cavity, three candidate formulations were identified by FACS that were sufficiently biocompatible in mice that they warranted investigation in a nonhuman primate. In primates, the larger 1.5 mm alginate spheres made from unmodified material did lead to fibrosis, displaying fibrotic overgrowth and dense myofibroblast coverage. Three modified candidate materials that were also evaluated in primates showed little to no fibrosis. A lead candidate was identified that was evaluated as a potential encapsulation system for stem cell-derived β -cells (SC-Islets) in immune-competent diabetic mice [113]. In these studies, three densities of SC-Islets were encapsulated in an alginate modified with thiomorpholine dioxide (TMTD). As demonstrated previously, SC-Islets encapsulated in 1.5-mm TMTD-alginate spheres showed enhanced performance compared to 0.5-mm spheres, which controlled glucose for only 15 days at the highest density. The 1.5-mm TMTD-alginate spheres controlled glucose for over 70 days at each of the densities tested, with much higher levels of human C-peptide.

Nanolayer shells of polyphenolic antioxidant materials are also being investigated as dual antioxidant and immunosuppressive ancillary encapsulation systems capable of reducing fibrosis [114]. The core-shell particles are produced by depositing hydrogen-bonded multilayers of polyphenol, poly(methacrylic acid) along with amino-containing poly(*N*-vinylpyrrolidone), or poly(*N*-vinylcaprolactam) onto silica particles. After deposition of four layers, the core can be removed, resulting in a hollow shell that can be coadministered with any number of encapsulation systems. The shells were shown to scavenge ROS generated by stimulation of OT-II splenic T cells with phorbol 12-myristate 12-acetate and ionomycin. TA shells were also effective in reducing the production of pro-inflammatory cytokines such as IFN- γ , TNF- α , and IL-2. Other polyphenolic compounds are in development for anti-fibrotic strategies, including the flavonoids taxifolin and quercitrin [115]. In an in vitro model comprised of human mesenchymal stem cells and human gingival fibroblasts, flavonoid-modified titanium surfaces demonstrated anti-fibrotic potential and increased differentiation of MSCs into osteoblasts.

Zwitterionic coatings have recently been developed as an alternative to traditional brush polymers, which are susceptible to coating loss in high shear

applications [116]. In general, hydrophilic coatings that are required on hydrophobic biomaterial substrates and permselective membranes can be eroded over time, gradually increasing the exposure of the hydrophobic material and the likelihood of membrane de-wetting. A zwitterionic macrocrosslinker has been developed as a polyurethane-grafted coating to provide better stability and long-term anti-fouling properties. In comparison to brush coatings, the addition of the macrocrosslinker retained the same low contact angle for up to 2 weeks in a flow cell, compared to only several days for the individual components. Protein fouling was also reduced by about sixfold. This type of coating strategy could be employed in many types of macroencapsulation devices, not only potentially improving anti-fibrotic properties but potentially improving the rate and stability of insulin and glucose transport kinetics.

Stem Cell-Derived B-Cells as an Alternative to Isolated Cadaveric Islets

In addition to the challenge of immunoprotection, cadaveric islet transplantation is limited by the scarcity of high-quality and consistent islet material. Both cause of death and islet isolation procedures and culture can negatively impact the performance of the tissue. Donor-to-donor variability is very high and has confounded development of clinical therapies. Thus, an alternative source has long been sought. Pluripotent embryonic stem cells (ESC), which were first isolated from human tissue in 1998 [117], are capable of expanding for dozens of generations and generating virtually all tissues of the body. This latter feature has meant that pluripotent stem cells could theoretically become the starting material for nearly infinite supplies of stem cell-derived β -cells to replace cadaveric islets as a transplantation source.

Although the idea was an obvious one, the path to achieve this goal has not been straightforward or rapid. In fact, since the derivation of the first ESC lines in 1998, it took 7 years to develop a robust method for inducing these cells to efficiently differentiate in the first step into endoderm tissue, based on molecular signals observed in the early development of model organisms like frogs, fish, and mice [118, 119]. This is the very first fate decision for ESCs, choosing between the three germ layers—ectoderm, mesoderm, or endoderm. The endodermal lineage forms the organs of the gut tube including the pancreas.

Generation of Glucoreponsive Stem Cell-Derived B-Cells

Following induction of the endodermal lineage, cells must be sequentially directed to differentiate into pancreatic specific progenitor cells [120, 121]. These cells could not be further differentiated to β -cells in vitro at the time, but they could be transplanted into rodents and over the course of several months undergo further differentiation in vivo to generate islet cell types, including a small population of β -cells, as

well as pancreatic ductal tissue. Though this *in vivo* differentiation process remains largely a black box even today, the fact that even some β -cells can be generated via this approach prompted Viacyste to proceed to clinical trials using stem cell-derived pancreatic progenitors in a macroencapsulation device [122]. One key challenge in the pancreatic progenitor step is to avoid the generation of progenitor cells for adjacent organ types along the gut tube, like the intestine or liver. Organ development and differentiation make repeated use of the same sets of signaling pathways, like retinoic acid or bone morphogenetic protein (BMP) pathway signaling [123]. The key to developing directed differentiation protocols is identifying precisely the right factors in the right combination for the right duration in the right sequence. This combinatorial challenge becomes even more difficult in the later stages of directed differentiation where the pathways and expression patterns in mice and humans diverge. Thus the last steps of directed differentiation from pancreatic progenitor cells to glucose-responsive insulin-secreting cells were particularly challenging and required empirical screening approaches. As a result, it took another 8 years following the first report of efficient stem cell-derived pancreatic progenitors in 2006 to the first reports of stem cell-derived β -cells (or β -like cells, SC- β -cells) in 2014 [124–126]. Today, these SC- β -cells (Fig. 2.7) are being developed by Semma Therapeutics.

These studies directed the differentiation of ESCs into pancreatic progenitors and then, using a combination of signaling pathways, induced those cells to differentiate into glucose-responsive insulin-secreting cells. A common theme of signaling pathways used for the final induction of β -cells was the combination of thyroid hormone signaling and TGF- β inhibition. The identification of this specific combination of signaling pathways was the result of empirical screening of many different pathways. Additional molecules have been added in certain protocols and cell lines to enhance maturation further including the calcium channel agonist BayK [126] and *N*-cysteine and AXL inhibition [125].

The most important feature of the cells produced by these techniques is their ability, for the first time, to secrete insulin in response to a glucose challenge. The generation of glucose-responsive insulin-secreting β -cells from stem cells has been a holy grail for this field for at least two decades. Importantly these cells

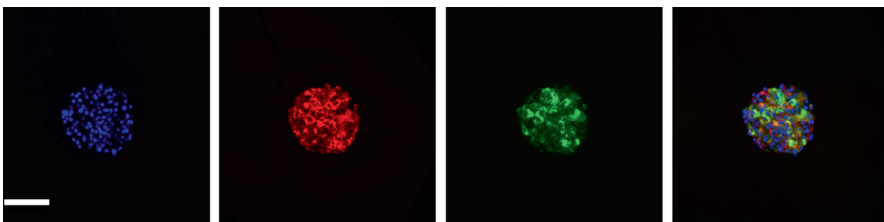


Fig. 2.7 SC-Islets produced by Semma Therapeutics. The *blue* signal is DAPI, staining nuclei. The *red* signal is chromogranin A, staining endocrine cells of the islet. The *green* signal is c-peptide, staining insulin-producing SC-beta cells. Scale bar = 100 μ m (Image courtesy of Yeh-Chuin Poh, Semma Therapeutics)

demonstrated this functional capacity both in vitro and in vivo, including the ability to provide glycemic control in diabetic animals. These achievements represent a turning point for the field in terms of its ability to generate islet cell types useful for drug screening, disease modeling, and ultimately cell therapy. Although this achievement was indisputably a major breakthrough, there remains a significant capacity for improvement in the efficiency of the protocols, the transferability across cell lines, and the ultimate functionality of the cells both in magnitude of insulin secreted and in reproducibility of the stimulation index (ratio of insulin secreted at high vs low glucose). In particular, in all cases published to date, these metrics for functionality were measurably less than for cadaveric human islets.

A second common theme of the published SC- β -cells is the expression of a number of β -cell-specific transcription factors, like Pdx1 and Nkx6.1, but not identical gene expression patterns to human islet β -cells. Some of these gene expression differences may be related to issues of genetic background or cause of death and methods of processing for the human islets. Alternatively, some of these gene and protein expression differences likely represent gaps in the complete differentiation or maturation of β -cells derived through an accelerated developmental process performed in the dish. Finally, most comparisons are made between SC- β -cells and adult human β -cells in cadaveric islets. A more appropriate comparison may be of neonatal or juvenile human islets, which may be closer in type and function to newly derived stem cell-derived islets. Nonetheless, ongoing and future improvements to protocols will likely move the expression patterns of these cells closer to that of endogenous tissue, whether adult or juvenile.

Clinical Translation of Stem Cell-Derived β -Cells

An obvious application of these newly described SC- β -cells is in cell transplantation for type 1 (or insulin-dependent type 2) diabetes. Given the ability of starting with a single pluripotent stem cell line of virtually unlimited expansion capacity, it should be possible to generate nearly unlimited supplies of standardized and qualified SC- β -cells for cell therapy. However, several key challenges exist in translating these initial academic discoveries into therapeutic candidates. These challenges include identifying clinically suitable starting cells lines and enhancing the differentiation protocols to produce cell product with appropriate composition, purity, and activity to move into clinical trials.

The choice of clinically suitable cell lines starts first with the identification of pluripotent cell lines that have been consented, documented, and derived in a manner consistent with FDA guidelines and preferably under xeno-free conditions. In addition, SC- β -cells have been generated from both embryonic stem cells (ESCs) and induced pluripotent stem cells (iPSC). ESC lines are derived from discarded blastocysts from in vitro fertilization clinics [117], and iPSC lines are derived from somatic tissue, like skin fibroblasts or peripheral blood, using the transient induction of exogenous pluripotency genes [127]. Although a number of trials are ongoing in the United States using ESC lines as starting material [128], none have begun

yet with iPSC lines in part due to the relative newness of the technology and in part due to technical questions related to the potential for acquisition of genetic mutations during reprogramming or the retention of exogenous reprogramming material. However, the first trial of an iPSC-derived product has started in Japan [129], and others are likely to follow. In addition to regulatory considerations and the choice of ESC vs iPSC, the most important features of a suitable line are its ability to expand through sufficient passages during manufacturing while maintaining phenotype and genotype and its ability to differentiate efficiently to the cell type of choice.

In addition to selecting suitable starting material, the other key challenge for clinical translation of SC- β -cells into the clinic is improving the efficiency of the differentiation protocols. This means improving the composition (increasing the number of β -like cells in the final mixture and potentially also increasing other islet cell types like the α - or γ -cells), improving the purity (removing any residual undifferentiated cells or cells that have differentiated into undesirable off-target lineages), and improving the potency (insulin content and stimulated release.) Each of these features is critical to a safe and effective cell product, and each individually is a challenging biological problem, raising the bar considerably from the first-generation protocols published in 2014. However, the ability to modulate these features through careful control of the developmental biology involved also present unprecedented opportunities for improving the cell product transplanted back into patients. For example, if high potency cell preparations can be developed, the ultimate dose for transplantation may be lessened, having a major impact on device volume requirements. Similarly, this *in vitro* process also provides multiple points in which to intervene to alter the ratios of cell types within the composition, which could impact long-term graft durability. Methods of genetically engineering the starting material in ways to achieve these or other design goals are certainly within reach, at least for first demonstration in preclinical proof of concept studies.

Finally, the key hurdle for the clinical translation of SC- β -cells is developing methods to safely deliver these cells to patients. These potential paths include immunosuppression-based approaches (substituting SC- β -cells for cadaveric islets) or autologous transplantation (making patient-specific SC- β -cells from patient iPSC lines). Both of these approaches are limited—the first by the limited patient population for whom the benefits outweigh the risks and the second by the logistical, manufacturing, and preclinical challenges to developing patient-specific therapies. Cells genetically engineered to be “invisible” to the immune system present another possible path, albeit with a lengthy and complicated path to clinical trials and unique risks.

The Future of β -Cell Therapy

Since the first demonstration that encapsulated islets could control hyperglycemia in animal models of diabetes, the field of cell encapsulation has evolved with the availability of new materials, new sources of islet tissue, and the scale of federal and private funding for encapsulation research and development. Achieving long-term

glycemic control with an encapsulated cell product remains a holy grail of cell therapy, impacted significantly by the reproducibility, reliability, and scale of available of cell sources. The viability and functionality of isolated primary islets can have a dramatic impact on the performance of encapsulation devices and can exacerbate or change the way that the host responds to these materials. One of the primary concerns of macrodevices is the nonspecific inflammatory response associated with the biomaterials that they are composed of. But limited access to a relevant number of islet cells required to recapitulate the requirements of a therapeutic dose for a human type 1 diabetic has contributed to poor translation from rodent models to the clinic, resulting from the inability to test encapsulation hypotheses empirically. While modeling is useful in predicting diffusive and oxygenation gradients within devices, the encapsulation process becomes quite different when encapsulating several million cells for a rodent compared to nearly a billion cells for a human. Stem cell-derived β -cells change that dynamic and for the first time may allow for the proper number and type of experiments to generate the empirical support required for human product development. With large-scale production of SC- β -cells on the horizon, the development of successful encapsulation approaches will be significantly accelerated, and the advances described in this chapter may serve as a road map toward several potential pathways to success.

References

1. Fullerton B, Jeitler K, Seitz M, Horvath K, Berghold A, Siebenhofer A. Intensive glucose control versus conventional glucose control for type 1 diabetes mellitus. *Cochrane Database Syst Rev* 2014;(2):CD009122.
2. Cryer PE, Davis SN, Shamoon H. Hypoglycemia in diabetes. *Diabetes Care*. 2003;26(6):1902–12.
3. Cryer PE. Hierarchy of physiological responses to hypoglycemia: relevance to clinical hypoglycemia in type I (insulin dependent) diabetes mellitus. *Horm Metab Res*. 1997;29(3):92–6.
4. Diedrich L, Sandoval D, Davis SN. Hypoglycemia associated autonomic failure. *Clin Auton Res*. 2002;12(5):358–65.
5. Gabrieli I, Shamoon H. Hypoglycemia in diabetes: common, often unrecognized. *Cleve Clin J Med*. 2004;71(4):335–42.
6. Pai CM, Bae YH, Mack EJ, Wilson DE, Kim SW. Concanavalin A microspheres for a self-regulating insulin delivery system. *J Pharm Sci*. 1992;81(6):532–6.
7. Bernkop-Schnurch A, Krauland A, Valenta C. Development and in vitro evaluation of a drug delivery system based on chitosan-EDTA BBI conjugate. *J Drug Target*. 1998;6(3):207–14.
8. Shah D, Shen WC. Transcellular delivery of an insulin-transferrin conjugate in enterocyte-like Caco-2 cells. *J Pharm Sci*. 1996;85(12):1306–11.
9. Russell SJ, El-Khatib FH, Sinha M, Magyar KL, McKeon K, Goergen LG, et al. Outpatient glycemic control with a bionic pancreas in type 1 diabetes. *N Engl J Med*. 2014;371:313–25.
10. Ricordi C. Completion of the first FDA phase III multicenter trial of islet transplantation in type 1 diabetes by the NIH CIT consortium severe hypoglycemia (hypo) and hypo unawareness. ISCT 2014, Paris.
11. Song SH, Kjems L, Ritzel R, McIntyre SM, Johnson ML, Veldhuis JD, et al. Pulsatile insulin secretion by human pancreatic islets. *J Clin Endocrinol Metab*. 2002;87:213–21.

12. FDA Approves MiniMed 670G System—World's First Hybrid Closed Loop System [press release]. <http://www.medtronicdiabetes.com/blog/fda-approves-minimed-670g-system-worlds-first-hybrid-closed-loop-system/2016>.
13. Administration FaD. Summary of safety and effectiveness data. http://www.accessdata.fda.gov/cdrh_docs/pdf16/P160017b.pdf2016.
14. Heinemann L, Fleming GA, Petrie JR, Holl RW, Bergenstal RM, Peters AL. Insulin pump risks and benefits: a clinical appraisal of pump safety standards, adverse event reporting, and research needs: a joint statement of the European Association for the Study of Diabetes and the American Diabetes Association Diabetes Technology Working Group. *Diabetes Care*. 2015;38(4):716–22.
15. Ellingsen C, Dassau E, Zisser H, Grosman B, Percival MW, Jovanovic L, et al. Safety constraints in an artificial pancreatic beta cell: an implementation of model predictive control with insulin on board. *J Diabetes Sci Technol*. 2009;3(3):536–44.
16. Kedia N. Treatment of severe diabetic hypoglycemia with glucagon: an underutilized therapeutic approach. *Diabetes Metab Syndr Obes*. 2011;4:337–46.
17. McCall AL, Farhy LS. Treating type 1 diabetes: from strategies for insulin delivery to dual hormonal control. *Minerva Endocrinol*. 2013;38(2):145–63.
18. Barton FB, Rickels MR, Alejandro R, Hering BJ, Wease S, Naziruddin B, et al. Improvement in outcomes of clinical islet transplantation: 1999–2010. *Diabetes Care*. 2012;35(7):1436–45.
19. Ricordi C, Goldstein JS, Balamurugan AN, Szot GL, Kin T, Liu C, et al. NIH-sponsored clinical islet transplantation consortium phase 3 trial: manufacture of a complex cellular product at eight processing facilities. *Diabetes*. 2016;65(11):3418–28.
20. Shapiro AM, Lakey JR, Ryan EA, Korbutt GS, Toth E, Warnock GL, et al. Islet transplantation in seven patients with type 1 diabetes mellitus using a glucocorticoid-free immunosuppressive regimen. *N Engl J Med*. 2000;343(4):230–8.
21. Korsgren O, Nilsson B, Berne C, Felldin M, Foss A, Kallen R, et al. Current status of clinical islet transplantation. *Transplantation*. 2005;79(10):1289–93.
22. Rickels MR, Liu C, Shlansky-Goldberg RD, Soleimanpour SA, Vivek K, Kamoun M, et al. Improvement in beta-cell secretory capacity after human islet transplantation according to the CIT07 protocol. *Diabetes*. 2013;62(8):2890–7.
23. Froud T, Baidal DA, Ponte G, Ferreira JV, Ricordi C, Alejandro R. Resolution of neurotoxicity and beta-cell toxicity in an islet transplant recipient following substitution of tacrolimus with MMF. *Cell Transplant*. 2006;15(7):613–20.
24. Administration FaD. Rapamune (Sirolimus) oral solution and tablets. http://www.fda.gov/ohrms/dockets/ac/02/briefing/3832b1_03_FDA-RapamuneLabel.htm2016.
25. Weir GC, Bonner-Weir S. Islets of Langerhans: the puzzle of intra-islet interactions and their relevance to diabetes. *J Clin Invest*. 1990;85(4):983–7.
26. Farmer TD, Jenkins EC, O'Brien TP, McCoy GA, Havlik AE, Nass ER, et al. Comparison of the physiological relevance of systemic vs. portal insulin delivery to evaluate whole body glucose flux during an insulin clamp. *Am J Physiol Endocrinol Metab*. 2015;308(3):E206–22.
27. Oliver JB, Beidas AK, Bongu A, Brown L, Shapiro ME. A comparison of long-term outcomes of portal versus systemic venous drainage in pancreatic transplantation: a systematic review and meta-analysis. *Clin Transpl*. 2015;29(10):882–92.
28. Lifson N, Kramlinger KG, Mayrand RR, Lender EJ. Blood flow to the rabbit pancreas with special reference to the islets of Langerhans. *Gastroenterology*. 1980;79(3):466–73.
29. Brissova M, Shostak A, Shiota M, Wiebe PO, Poffenberger G, Kantz J, et al. Pancreatic islet production of vascular endothelial growth factor—a is essential for islet vascularization, revascularization, and function. *Diabetes*. 2006;55(11):2974–85.
30. Andersson A, Korsgren O, Jansson L. Intraportally transplanted pancreatic islets revascularized from hepatic arterial system. *Diabetes*. 1989;38(Suppl 1):192–5.
31. Lau J, Jansson L, Carlsson PO. Islets transplanted intraportally into the liver are stimulated to insulin and glucagon release exclusively through the hepatic artery. *Am J Transplant*. 2006;6(5 Pt 1):967–75.

32. Henriksnas J, Lau J, Zang G, Berggren PO, Kohler M, Carlsson PO. Markedly decreased blood perfusion of pancreatic islets transplanted intraportally into the liver: disruption of islet integrity necessary for islet revascularization. *Diabetes*. 2012;61(3):665–73.
33. Kim HI, JE Y, Park CG, Kim SJ. Comparison of four pancreatic islet implantation sites. *J Korean Med Sci*. 2010;25(2):203–10.
34. Pepper AR, Gala-Lopez B, Pawlick R, Merani S, Kin T, Shapiro AM. A prevascularized subcutaneous device-less site for islet and cellular transplantation. *Nat Biotechnol*. 2015;33(5):518–23.
35. Henderson JR, Moss MC. A morphometric study of the endocrine and exocrine capillaries of the pancreas. *Q J Exp Physiol*. 1985;70(3):347–56.
36. Olsson R, Carlsson PO. The pancreatic islet endothelial cell: emerging roles in islet function and disease. *Int J Biochem Cell Biol*. 2006;38(4):492–7.
37. Lammert E, Gu G, McLaughlin M, Brown D, Brekken R, Murtaugh LC, et al. Role of VEGF-A in vascularization of pancreatic islets. *Curr Biol*. 2003;13(12):1070–4.
38. Toyofuku Y, Uchida T, Nakayama S, Hirose T, Kawamori R, Fujitani Y, et al. Normal islet vascularization is dispensable for expansion of beta-cell mass in response to high-fat diet induced insulin resistance. *Biochem Biophys Res Commun*. 2009;383(3):303–7.
39. Buchwald P. FEM-based oxygen consumption and cell viability models for avascular pancreatic islets. *Theor Biol Med Model*. 2009;6:5.
40. Balaji S, Mcquilling JP, Khanna O, Brey EM, Opara EC. Chpt 14: Vascularization of encapsulated cells. New York: CRC Press; 2012. p. 283–300.
41. Tomei AA, Manzoli V, Fraker CA, Giraldo J, Velluto D, Najjar M, et al. Device design and materials optimization of conformal coating for islets of Langerhans. *Proc Natl Acad Sci U S A*. 2014;111:10514–9.
42. Yamamoto T, Ricordi C, Messinger S, Sakuma Y, Miki A, Rodriguez R, et al. Deterioration and variability of highly purified collagenase blends used in clinical islet isolation. *Transplantation*. 2007;84(8):997–1002.
43. Brandhorst H, Brandhorst D, Hering BJ, Federlin K, Bretzel RG. Body mass index of pancreatic donors: a decisive factor for human islet isolation. *Exp Clin Endocrinol Diabetes*. 1995;103(Suppl 2):23–6.
44. Wang Y, Danielson KK, Ropski A, Harvat T, Barbaro B, Paushter D, et al. Systematic analysis of donor and isolation factor's impact on human islet yield and size distribution. *Cell Transplant*. 2013;22(12):2323–33.
45. Chen W, Lisowski M, Khalil G, Sweet IR, Shen AQ. Microencapsulated 3-dimensional sensor for the measurement of oxygen in single isolated pancreatic islets. *PLoS One*. 2012;7(3):e33070.
46. Gorbet MB, Sefton MV. Biomaterial-associated thrombosis: roles of coagulation factors, complement, platelets and leukocytes. *Biomaterials*. 2004;25(26):5681–703.
47. Fischer M, Sperling C, Tengvall P, Werner C. The ability of surface characteristics of materials to trigger leukocyte tissue factor expression. *Biomaterials*. 2010;31(9):2498–507.
48. Franz S, Rammelt S, Scharnweber D, Simon JC. Immune responses to implants—a review of the implications for the design of immunomodulatory biomaterials. *Biomaterials*. 2011;32(28):6692–709.
49. Bygd HC, Forsmark KD, Bratlje KM. Altering in vivo macrophage responses with modified polymer properties. *Biomaterials*. 2015;56:187–97.
50. Deonaraine K, Panelli MC, Stashower ME, Jin P, Smith K, Slade HB, et al. Gene expression profiling of cutaneous wound healing. *J Transl Med*. 2007;5:11.
51. Fukano Y, Usui ML, Underwood RA, Isenhath S, Marshall AJ, Hauch KD, et al. Epidermal and dermal integration into sphere-templated porous poly(2-hydroxyethyl methacrylate) implants in mice. *J Biomed Mater Res A*. 2010;94(4):1172–86.
52. Madden LR, Mortisen DJ, Sussman EM, Dupras SK, Fugate JA, Cuy JL, et al. Proangiogenic scaffolds as functional templates for cardiac tissue engineering. *Proc Natl Acad Sci U S A*. 2010;107(34):15211–6.

53. Saino E, Focarete ML, Gualandi C, Emanuele E, Cornaglia AI, Imbriani M, et al. Effect of electrospun fiber diameter and alignment on macrophage activation and secretion of proinflammatory cytokines and chemokines. *Biomacromolecules*. 2011;12:1900–11.
54. Paul NE, Skazik C, Harwardt M, Bartneck M, Denecke B, Klee D, et al. Topographical control of human macrophages by a regularly microstructured polyvinylidene fluoride surface. *Biomaterials*. 2008;29:4056–64.
55. Kanak MA, Takita M, Kunnathodi F, Lawrence MC, Levy MF, Naziruddin B. Inflammatory response in islet transplantation. *Int J Endocrinol*. 2014;2014:451035.
56. Hume PS, Anseth KS. Polymerizable superoxide dismutase mimetic protects cells encapsulated in poly(ethylene glycol) hydrogels from reactive oxygen species-mediated damage. *J Biomed Mater Res A*. 2011;99(1):29–37.
57. Chen T, Yuan J, Duncanson S, Hibert ML, Kodish BC, Mylavaganam G, et al. Alginate encapsulant incorporating CXCL12 supports long-term allo- and xenoislet transplantation without systemic immune suppression. *Am J Transplant*. 2015;15:618–27.
58. Helton KL, Ratner BD, Wisniewski NA. Biomechanics of the sensor-tissue interface-effects of motion, pressure, and design on sensor performance and foreign body response-part II: examples and application. *J Diabetes Sci Technol*. 2011;5(3):647–56.
59. Zeman LJ, Zydney AL. Microfiltration and ultrafiltration: principles and applications. New York: M. Dekker; 1996. xix, 618 p
60. Gray DW. An overview of the immune system with specific reference to membrane encapsulation and islet transplantation. *Ann N Y Acad Sci*. 2001;944:226–39.
61. Iwata H, Morikawa N, Fujii T, Takagi T, Samejima T, Ikada Y. Does immunoisolation need to prevent the passage of antibodies and complements? *Transplant Proc*. 1995;27(6):3224–6.
62. Perkins SJ. Molecular modelling of human complement subcomponent C1q and its complex with C1r2C1s2 derived from neutron-scattering curves and hydrodynamic properties. *Biochem J*. 1985;228(1):13–26.
63. Silverton EW, Navia MA, Davies DR. Three-dimensional structure of an intact human immunoglobulin. *Proc Natl Acad Sci U S A*. 1977;74(11):5140–4.
64. Krishnan L, Clayton LR, Boland ED, Reed RM, Hoying JB, Williams SK. Cellular immunoisolation for islet transplantation by a novel dual porosity electrospun membrane. *Transplant Proc*. 2011;43(9):3256–61.
65. RF, PP, Inventors. Gen Electric, assignee. Process for making cylindrical holes in a sheet material. USA; 1974.
66. Calvo JI, Hernández A, Prádanos P, Martibnez L, Bowen WR. Pore size distributions in microporous membranes: II. Bulk characterization of track-etched filters by air porometry and mercury porosimetry. *J Colloid Interface Sci* 1995;(176):467–78.
67. Song S, Faleo G, Yeung R, Kant R, Posselt AM, Desai TA, et al. Silicon nanopore membrane (SNM) for islet encapsulation and immunoisolation under convective transport. *Sci Rep*. 2016;6:23679.
68. Desai TA, Hansford DJ, Leoni L, Essenpreis M, Ferrari M. Nanoporous anti-fouling silicon membranes for biosensor applications. *Biosens Bioelectron*. 2000;15(9–10):453–62.
69. Nyitray CE, Chang R, Faleo G, Lance KD, Bernards DA, Tang Q, et al. Polycaprolactone thin-film micro- and nanoporous cell-encapsulation devices. *ACS Nano*. 2015;9(6):5675–82.
70. Neufeld T, Ludwig B, Barkai U, Weir GC, Colton CK, Evron Y, et al. The efficacy of an immunoisolating membrane system for islet xenotransplantation in minipigs. *PLoS One*. 2013;8(8):e70150.
71. Lavin DM, Bintz BE, Thanos CG. The diffusive properties of hydrogel microcapsules for cell encapsulation. *Methods Mol Biol*. 2017;1479:119–34.
72. Trivedi N, Keegan M, Steil GM, Hollister-Lock J, Hasenkamp WM, Colton CK, et al. Islets in alginate macrobeads reverse diabetes despite minimal acute insulin secretory responses. *Transplantation*. 2001;71(2):203–11.
73. Martinsen A SI, Skjærk-Braek G. Alginate as immobilization material: III. Diffusional properties. *Biotechnol Bioeng*. 1992;39:186–94.

74. Bosco D, Armanet M, Morel P, Niclauss N, Sgroi A, Muller YD, et al. Unique arrangement of alpha- and beta-cells in human islets of Langerhans. *Diabetes*. 2010;59(5):1202–10.
75. Colton CK. Oxygen supply to encapsulated therapeutic cells. *Adv Drug Deliv Rev*. 2014;67–68:93–110.
76. Papas KK, Avgoustiniatos ES, Suszynski TM. Effect of oxygen supply on the size of implantable islet-containing encapsulation devices. *Panminerva Med*. 2016;58(1):72–7.
77. Dionne KE, Colton CK, Yarmush ML. Effect of hypoxia on insulin secretion by isolated rat and canine islets of Langerhans. *Diabetes*. 1993;42(1):12–21.
78. Pisania A, Weir GC, O'Neil JJ, Omer A, Tchipashvili V, Lei J, et al. Quantitative analysis of cell composition and purity of human pancreatic islet preparations. *Lab Invest*. 2010;90(11):1661–75.
79. Araki J, Kato H, Doi K, Kuno S, Kinoshita K, Minoda K, et al. Application of normobaric hyperoxygenation to an ischemic flap and a composite skin graft. *Plast Reconstr Surg Glob Open*. 2014;2:e152.
80. Barkai U, Rotem A, de Vos P. Survival of encapsulated islets: more than a membrane story. *World J Transplant*. 2016;6(1):69–90.
81. Papas KK, Bellin MD, Sutherland DER, Suszynski TM, Kitzmann JP, Avgoustiniatos ES, et al. Islet oxygen consumption rate (OCR) dose predicts insulin independence in clinical islet autotransplantation. *PLoS One*. 2015;10(8):e0134428.
82. Papas KK, Colton CK, Nelson RA, Rozak PR, Avgoustiniatos ES, Scott WE 3rd, et al. Human islet oxygen consumption rate and DNA measurements predict diabetes reversal in nude mice. *Am J Transplant*. 2007;7(3):707–13.
83. Papas KK, Colton CK, Qipo A, Wu H, Nelson RA, Hering BJ, et al. Prediction of marginal mass required for successful islet transplantation. *J Invest Surg*. 2010;23(1):28–34.
84. Gilbert M, Jung SR, Reed BJ, Sweet IR. Islet oxygen consumption and insulin secretion tightly coupled to calcium derived from L-type calcium channels but not from the endoplasmic reticulum. *J Biol Chem*. 2008;283(36):24334–42.
85. Jackson R, Togtema M, Lambert PF, Zehbe I. Tumorigenesis driven by the human papillomavirus type 16 Asian-American e6 variant in a three-dimensional keratinocyte model. *PLoS One*. 2014;9(7):e101540.
86. Ludwig B, Reichel A, Steffen A, Zimmerman B, Schally AV, Block NL, et al. Transplantation of human islets without immunosuppression. *Proc Natl Acad Sci U S A*. 2013;110:1–5.
87. Dolgin E. Diabetes: encapsulating the problem. *Nature*. 2016;540(7632):S60–2.
88. Nose Y. Oxygen-carrying macromolecules: therapeutic agents for the treatment of hypoxia. *Artif Organs*. 1998;22(7):618–22.
89. Farrar D, Grocott M. Intravenous artificial oxygen carriers. *Hosp Med*. 2003;64(6):352–6.
90. Johnson AS, O'Sullivan E, D'Aoust LN, Omer A, Bonner-Weir S, Fisher RJ, et al. Quantitative assessment of islets of Langerhans encapsulated in alginate. *Tissue Eng Part C Methods*. 2011;17(4):435–49.
91. Gattas-Asfura KM, Fraker CA, Stabler CL. Perfluorinated alginate for cellular encapsulation. *J Biomed Mater Res A*. 2012;100(8):1963–71.
92. Cassidy DP, Irvine RL. Use of calcium peroxide to provide oxygen for contaminant biodegradation in a saturated soil. *J Hazard Mater*. 1999;69(1):25–39.
93. Wang J, Zhu Y, Bawa HK, Ng G, Wu Y, Libera M, et al. Oxygen-generating nanofiber cell scaffolds with antimicrobial properties. *ACS Appl Mater Interfaces*. 2011;3(1):67–73.
94. SH O, Ward CL, Atala A, Yoo JJ, Harrison BS. Oxygen generating scaffolds for enhancing engineered tissue survival. *Biomaterials*. 2009;30(5):757–62.
95. Pedraza E, Coronel MM, Fraker CA, Ricordi C, Stabler CL. Preventing hypoxia-induced cell death in beta cells and islets via hydrolytically activated, oxygen-generating biomaterials. *Proc Natl Acad Sci U S A*. 2012;109(11):4245–50.
96. McQuilling JP, Opara EC. Methods for incorporating oxygen-generating biomaterials into cell culture and microcapsule systems. *Methods Mol Biol*. 2017;1479:135–41.

97. Montazeri L, Hojjati-Emami S, Bonakdar S, Tahamtani Y, Hajizadeh-Saffar E, Noori-Keshtkar M, et al. Improvement of islet engrafts by enhanced angiogenesis and microparticle-mediated oxygenation. *Biomaterials*. 2016;89:157–65.
98. Duling BR, Berne RM. Longitudinal gradients in periarteriolar oxygen tension. A possible mechanism for the participation of oxygen in local regulation of blood flow. *Circ Res*. 1970;27(5):669–78.
99. Pittman RN. Regulation of tissue oxygenation. *Integrated systems physiology: from molecule to function to disease*. San Rafael, CA: Morgan & Claypool Life Sciences; 2011.
100. Geller RL, Loudovaris T, Neuenfeldt S, Johnson RC, Brauker JH. Use of an immunoisolation device for cell transplantation and tumor immunotherapy. *Ann N Y Acad Sci*. 1997;831:438–51.
101. Rafael E, Wernerson A, Arner P, Tibell A. In vivo studies on insulin permeability of an immunoisolation device intended for islet transplantation using the microdialysis technique. *Eur Surg Res*. 1999;31(3):249–58.
102. Rafael E, Wernerson A, Arner P, Wu GS, Tibell A. In vivo evaluation of glucose permeability of an immunoisolation device intended for islet transplantation: a novel application of the microdialysis technique. *Cell Transplant*. 1999;8(3):317–26.
103. Rafael E, Gazelius B, Wu GS, Tibell A. Longitudinal studies on the microcirculation around the TheraCyte immunoisolation device, using the laser Doppler technique. *Cell Transplant*. 2000;9(1):107–13.
104. Rafael E, Wu GS, Hultenby K, Tibell A, Wernerson A. Improved survival of macroencapsulated islets of Langerhans by preimplantation of the immunoisolating device: a morphometric study. *Cell Transplant*. 2003;12(4):407–12.
105. Sorenby AK, Kumagai-Braesch M, Sharma A, Hultenby KR, Wernerson AM, Tibell AB. Preimplantation of an immunoprotective device can lower the curative dose of islets to that of free islet transplantation: studies in a rodent model. *Transplantation*. 2008;86(2):364–6.
106. Pileggi A, Molano RD, Ricordi C, Zahr E, Collins J, Valdés-González RA, et al. Reversal of diabetes by pancreatic islet transplantation into a subcutaneous, neovascularized device. *Transplantation*. 2006;81:1318–24.
107. Pepper AR, Dinyari P, Malcolm AJ, Kin T, Pawlick LR, Senior PA. Subcutaneous clinical islet transplantation in a prevascularized subcutaneous pouch—preliminary experience. *CellR4*. 2016;4:1–10.
108. Pepper AR, Pawlick R, Bruni A, Gala-Lopez B, Wink J, Rafiei Y, et al. Harnessing the foreign body reaction in marginal mass device-less subcutaneous islet transplantation in mice. *Transplantation*. 2016;100(7):1474–9.
109. Anderson JM, Rodriguez A, Chang DT. Foreign body reaction to biomaterials. *Semin Immunol*. 2008;20(2):86–100.
110. Tibell A, Rafael E, Wennberg L, Nordenstrom J, Bergstrom M, Geller RL, et al. Survival of macroencapsulated allogeneic parathyroid tissue one year after transplantation in nonimmunosuppressed humans. *Cell Transplant*. 2001;10(7):591–9.
111. Veisheh O, Doloff JC, Ma M, Vegas AJ, Tam HH, Bader AR, et al. Size- and shape-dependent foreign body immune response to materials implanted in rodents and non-human primates. *Nat Mater*. 2015;14:643–51.
112. Vegas AJ, Veisheh O, Doloff JC, Ma M, Tam HH, Bratlie K, et al. Combinatorial hydrogel library enables identification of materials that mitigate the foreign body response in primates. *Nat Biotechnol*. 2016;34(3):345–52.
113. Vegas AJ, Veisheh O, Gürtler M, Millman JR, Pagliuca FW, Bader AR, et al. Long-term glycemic control using polymer-encapsulated human stem cell-derived beta cells in immune-competent mice. *Nat Med*. 2016;22(3):306–11.
114. Kozlovskaya V, Xue B, Lei W, Padgett LE, Tse HM, Kharlampieva E. Hydrogen-bonded multilayers of tannic acid as mediators of T-cell immunity. *Adv Healthc Mater*. 2015;4(5):686–94.
115. Cordoba A, Satue M, Gomez-Florit M, Hierro-Oliva M, Petzold C, Lyngstadaas SP, et al. Flavonoid-modified surfaces: multifunctional bioactive biomaterials with osteopromotive, anti-inflammatory, and anti-fibrotic potential. *Adv Healthc Mater*. 2015;4(4):540–9.

116. Wang W, Lu Y, Xie J, Zhu H, Cao Z. A zwitterionic macro-crosslinker for durable non-fouling coatings. *Chem Commun (Camb)*. 2016;52(25):4671–4.
117. Thomson JA, Itskovitz-Eldor J, Shapiro SS, Waknitz MA, Swiergiel JJ, Marshall VS, et al. Embryonic stem cell lines derived from human blastocysts. *Science*. 1998;282(5391):1145–7.
118. Kim SK, Hebrok M, Li E, Oh SP, Schrewe H, Harmon EB, et al. Activin receptor patterning of foregut organogenesis. *Genes Dev*. 2000;14(15):1866–71.
119. D'Amour KA, Agulnick AD, Eliazar S, Kelly OG, Kroon E, Baetge EE. Efficient differentiation of human embryonic stem cells to definitive endoderm. *Nat Biotechnol*. 2005;23(12):1534–41.
120. Hebrok M, Kim SK, Melton DA. Notochord repression of endodermal Sonic hedgehog permits pancreas development. *Genes Dev*. 1998;12(11):1705–13.
121. D'Amour KA, Bang AG, Eliazar S, Kelly OG, Agulnick AD, Smart NG, et al. Production of pancreatic hormone-expressing endocrine cells from human embryonic stem cells. *Nat Biotechnol*. 2006;24(11):1392–401.
122. Viacyste. A safety, tolerability, and efficacy study of VC-01™ combination product in subjects with type I diabetes mellitus <https://clinicaltrials.gov/ct2/show/NCT02239354>2014.
123. McCracken KW, Wells JM. Molecular pathways controlling pancreas induction. *Semin Cell Dev Biol*. 2012;23(6):656–62.
124. Pagliuca FW, Millman JR, Gürtler M, Segel M, Van Dervort A, Ryu JH, et al. Generation of functional human pancreatic? Cells in vitro. *Cell*. 2014;159:428–39.
125. Rezaania A, Bruin JE, Arora P, Rubin A, Batushansky I, Asadi A, et al. Reversal of diabetes with insulin-producing cells derived in vitro from human pluripotent stem cells. *Nat Biotechnol*. 2014;32(11):1121–33.
126. Russ HA, Parent AV, Ringler JJ, Hennings TG, Nair GG, Shveygert M, et al. Controlled induction of human pancreatic progenitors produces functional beta-like cells in vitro. *EMBO J*. 2015;34(13):1759–72.
127. Takahashi K, Yamanaka S. Induction of pluripotent stem cells from mouse embryonic and adult fibroblast cultures by defined factors. *Cell*. 2006;126(4):663–76.
128. Alper J. Geron gets green light for human trial of ES cell-derived product. *Nat Biotechnol*. 2009;27(3):213–4.
129. Cyranoski D. Japanese woman is first recipient of next-generation stem cells. *Nature*. 2014; doi:10.1038/nature.2017.21730.

Cell Therapy

Current Status and Future Directions

Emerich, D.F.; Orive, G. (Eds.)

2017, XVI, 328 p. 59 illus., 49 illus. in color., Hardcover

ISBN: 978-3-319-57152-2

A product of Humana Press